PHYSICO-MECHANICAL AND PETROGRAPHIC ANALYSIS OF MANSEHRA GRANITE, HAZARA BASIN, PAKISTAN

SULEMAN GUL KHAN

09-262242-019

BAHRIA UNIVERSITY ISLAMABAD

PHYSICO-MECHANICAL AND PETROGRAPHIC ANALYSIS OF MANSEHRA GRANITE, HAZARA BASIN, PAKISTAN

SULEMAN GUL KHAN

09-262242-019

A thesis is submitted in fulfillment of the requirement for the award of the degree of Master of Science (Geology)

Department of Earth and Environmental Sciences

BAHRIA UNIVERSITY ISLAMABAD

OCTOBER 2026

Bahria University

Department of Earth & Environmental Sciences

Islamabad Campus, Islamabad

Date: October 06, 2026

Certificate

A thesis submitted by **Mr. Suleman Gul Khan** to the Department of Earth & Environmental Sciences, Bahria University, Islamabad in partial fulfillment of the requirements for the degree of **Master of Science in Geology** (Session **2024– 2026**).

Committee Members	Name	Signature
Supervisor	Dr. Mumtaz Ali Khan	
Co-Supervisor	Mr. Masood Anwar	
Internal Examiner	Dr. Adeeb Ahmed	
External Examiner	Dr. Muhammad Sajid	
Post Graduate Coordinator	Dr. Adeeb Ahmed	
Head of Department (E&ES)	Dr. Syed Umair Ullah Jamil	

APPROVAL OF EXAMINATION

Scholar's Name: "Suleman Gul Khan"

Registration No: "67105"

Program of Study: MS Geology

Thesis Title: "PHYSICO-MECHANICAL AND PETROGRAPHIC ANALYSIS OF MANSEHRA GRANITE, HAZARA BASIN, PAKISTAN"

It is to certify that the above scholar's thesis has been completed to my satisfaction and to my belief, its standard is appropriate for submission for examination. I have also conducted plagiarism test of this thesis using HEC prescribed software and found similarity index 15% that is within the permissible limit set by the HEC for the MS degree thesis. I have also found the thesis in a format recognized by the BU for the MS thesis.

NOTE: The Plagiarism report is attached at the end of thesis.

Supervisor's Signature:_____

Date:

Name: Dr. Mumtaz Ali Khan

AUTHOR'S DECLERATION

I, "Mr. Suleman Gul Khan" is hereby stating that my MS thesis titled "PHYSICO-MECHANICAL AND PETROGRAPHIC ANALYSIS OF MANSEHRA GRANITE, HAZARA BASIN, PAKISTAN" is my own work and has not been submitted previously by me of taking any degree from this university "Bahria University Islamabad Campus" or anywhere else in the country/world.

At any time if my statement is found to be incorrect even after my graduation, the University has the right to withdraw/cancel my MS degree.

Scholar Name: Suleman Gul Khan

Sign: _____

Date:

PLAGIARISM UNDERTAKING

I solemnly declare that research work presented in the thesis titled "PHYSICO-MECHANICAL AND PETROGRAPHIC ANALYSIS OF MANSEHRA GRANITE, HAZARA BASIN, PAKISTAN" is solely my research work with no significant contribution from any other person. Small contribution/help wherever taken has been duly acknowledged and that complete thesis has been written by me.

I understand the zero-tolerance policy of HEC and Bahria University towards plagiarism. Therefore, I as an Author of the above titled thesis declared that no portion of my thesis has been plagiarized, and any material used as reference is properly referred/ cited.

I understand that if, I am found guilty of any formal plagiarism in the above titled thesis even after award of MS degree, the university reserves the right to withdraw, revoke my MS degree and that HEC and the University has the right to publish my name on the HEC/University website on which names of the scholars are placed who submitted plagiarized thesis.

Scholar/Author's

Sign: _____

Name of the Scholar: Suleman Gul Khan

DEDICATION

This thesis is dedicated to my family

ACKNOWLEDGEMENT

All praise and gratitude are owed to Almighty Allah, whose boundless mercy and guidance made the completion of this research possible.

I am deeply grateful to my supervisor, Dr. Mumtaz Ali Khan, Associate Professor in the Department of Earth and Environmental Sciences at Bahria University, H-11 Campus, Islamabad, for his expert guidance, mentorship, and continuous intellectual support throughout this research. His valuable feedback and dedication to academic excellence greatly shaped this thesis and enriched my understanding of the field. I am also very grateful to my Co-Supervisor, Mr. Masood Anwar, Assistant Professor in the Department of Earth and Environmental Sciences at Bahria University, for his guidance and efforts regarding laboratory analysis at Bahria University. I also extend my sincere thanks to the Tunneling Institute of Pakistan for facilitating the Schmidt Rebound Hammer testing, Bahria University for providing access to Uniaxial Compressive Strength testing, and thin section preparation, and lastly to National Museum of Natural History Islamabad for facilitation of petrography, all of which were essential to the analytical component of this study.

My heartfelt gratitude goes to my parents and family for their unconditional love, prayers, and unwavering support, which have been the cornerstone of my academic journey. Finally, I sincerely acknowledge all individuals who contributed in any capacity to the successful completion of this thesis.

ABSTRACT

The Mansehra Granitic Complex of the Hazara Basin, northern Pakistan, represents a critical lithological unit whose geotechnical properties have direct implications for infrastructure development, slope stability assessment, and rock engineering across the tectonically active Himalayan foreland. This study presents an integrated petrographic and geotechnical characterization of six granite specimens (S1–S6) collected from the complex, correlating modal mineralogy derived from visual estimation of petrography with two primary rock strength parameters; Uniaxial Compressive Strength (UCS) and Schmidt Rebound Hardness (SRH). UCS values across the six samples ranged from 124 MPa (S2) to 150 MPa (S1), while SRH values ranged from 52 MPa to 71 MPa, placing all specimens within the Strong to Very strong and High rock categories as per (GS, 1977, IAEG, 1977 and ISRM, 1978) classifications. Modal analysis revealed quartz contents of 45–66%, cumulative felsic indices (quartz + total feldspar) of 72–88%, and biotite contents of 4–18% across the sample set. Regression analysis demonstrated a strong positive correlation between SRH and UCS ($R^2 = 0.9328$), confirming Schmidt hammer reliability as a field strength proxy for this lithology. UCS correlated strongly with the cumulative petrographic index ($R^2 = 0.8276$), with higher felsic proportions consistently yielding greater compressive strength. The SRH vs Petrography regression produced a moderate R^2 of 0.6462, attributable to surface scale effects inherent to the Schmidt hammer test. Specimen dominated by K-feldspar and quartz (notably S1: 88% cumulative felsic, 29% K-feldspar) exhibited the greatest strength, while biotite rich, feldspar depleted specimen (S2: 72% cumulative felsic, 18% biotite) showed the lowest. These findings establish that Mansehra Granite is a very strong rock but due to the sample pool being limited to six (6) samples the correlation and regression analysis must be further validated by increasing the number of samples.

TABLE OF CONTENTS

CHAPTER NO.	TITLE	PAGE NO.
	APPROVAL OF EXAMINATION	i
	AUTHOR'S DECLARATION	ii
	PLAGIARISM UNDERTAKING	iii
	DEDICATION	iv
	ACKNOWLEDGEMENT	v
	ABSTRACT	vi
	LIST OF TABLES	xi
	LIST OF FIGURES	xiii
	LIST OF ABBREVIATIONS	xvii
1	**INTRODUCTION**	1
	1.1 Background	1
	1.2 Rock and Soil Mechanics	3
	1.2.1 Rock strength and its measurement	3

1.2.2 Factors controlling rock strength 4

1.2.3 Rock mass Classification systems 5

1.3 Importance of engineering geology 6

1.4 Significance of the study 7

1.5 Literature review 7

1.5.1 Research gap 9

1.6 Research Question(s) 9

1.6.1 Objectives 9

2 GEOLOGY AND TECTONICS 11

2.1 Regional geology 11

2.2 Structural framework 12

2.3 Stratigraphy of the Hazara Basin 13

2.3.1 The Mansehra Granitic Complex 15

3 METHODOLOGY 17

3.1 Work methodology 17

3.1.1 Thin section preparation 23

3.1.2 Petrographic analysis 24

3.1.3 Schmidt Rebound Hammer (Indirect-ASTM D 5873-00 26

3.1.4 Uniaxial Compressive Strength Test (Direct-ASTM D 2938-95) 31

4 RESULTS AND INTERPRETATION 35

4.1 Mechanical tests results 35

4.1.1 Uniaxial Compressive Strength (UCS) 35

4.1.2 Schmidt Rebound Hammer (SRH) 36

4.2 Petrographic analysis 37

5 DISCUSSION 45

5.1 Discussion 45

5.1.1 Correlation of mechanical tests with standards 45

5.1.2 Correlation of mechanical tests with petrography 50

5.1.3 Influence of petrographic variability on geotechnical performance 53

5.1.4 Regression analysis 53

CONCLUSIONS 57

RECOMMENDATIONS 59

REFERENCES 60

LIST OF TABLES

TABLE NO.	TITLE	PAGE NO.
2.1	Generalized Stratigraphy of Mansehra region, the table shows formations from the Precambrian to recent with the formation of interest highlighted in green (Awan et al., 2021)	14
3.1	Coordinates of the Samples of Mansehra Granite	21
3.2	Generalized magnification scheme for objective lens	27
4.1	Results of uniaxial compressive strength test of Mansehra Granite	36
4.2	Schmidt rebound hammer test results of Mansehra Granite	37
4.3	Modal mineralogy of Mansehra Granite	40
5.1	Standards of measurements for mechanical tests (Geological Society, 1977; IAEG, 1977; ISRM, 1981)	47
5.2	UCS Test results of Mansehra Granite correlation with standard (Geological Society, 1977; IAEG, 1977; ISRM, 1981)	48

5.3	SRH test results of Mansehra Granite correlated with standard (Geological Society, 1977; IAEG, 1977; ISRM, 1981)	48
5.4	Correlation Between UCS and SRH of Mansehra Granite	49
5.5	Modal mineralogy, UCS and SRH data of Mansehra Granite	51

LIST OF FIGURES

FIGURE NO.	TITLE	PAGE NO.
1.1	Location map of the study area showing District Mansehra (highlighted in blue color and marked by red) from where sampling was done, Khyber Pakhtunkhwa, Pakistan (ArcMap 10.5)	2
2.1	A geological map of the Hazara Basin depicting the spatial distribution of key rock units and geographic features, including; (1) Cambrian–Ordovician Mansehra Granite, (2) Meso-Neoproterozoic Tanawal Formation, (3) Paleoproterozoic Metamorphic Rocks, (4) Mesoproterozoic Hazara Formation, (5) Neoproterozoic–Cambrian sequences, (6) Jurassic; (7) Cretaceous, (8) Quaternary, (9) Paleogene, (10) Roads, (11) Rivers and Reservoirs, (12) Cities, Towns, and Villages, and the red box highlights the Study Area (after Iqbal et al., 2026)	11
3.1	Adapted methodology for this study	20
3.2	Photograph of the bulk specimens taken during fieldwork of Mansehra Granite	21

3.3	Bulk specimens sampling location map of Mansehra Granite (ArcMap 10.5)	22
3.4	Coring of bulk specimens of Mansehra Granite	23
3.5	Secured core specimens from bulk samples of Mansehra Granite	23
3.6	Slab preparation from core specimens at Bahria University Islamabad	25
3.7	Polarized microscope at geoscience lab of National Museum of Natural History, Islamabad	26
3.8	Generalized schematics of SRH	28
3.9	Graph for rebound value estimation	29
3.10	Generalized steps of SRH testing	30
3.11	Tunneling institute of Pakistan (Lab site where SRH tests were performed)	30
3.12	Cylindrical core specimen's definitions of stress conditions and strains (ASTM D 2938-95)	31
3.13	Performing UCS test on core 1 of Mansehra Granite	33
3.14	Performing UCS test on core 5 of Mansehra Granite	33

3.15	Performing UCS test on core 6 of Mansehra Granite	34
4.1	Representative photomicrographs of sample no. 1, (0.5mm), XPL, showing higher quartz and feldspar content with alteration of biotite and oxidation	41
4.2	Representative photomicrographs of sample no. 2, 0.5mm, XPL, showing more prominent opaques and biotite alteration with cleavage traces which control mechanical anisotropy	41
4.3	Representative photomicrographs of sample no. 3, 0.5mm, XPL, showing visible fractures, strained quartz grains, biotite grains with visible parallel cleavages, and extensive oxidation	42
4.4	Representative photomicrographs of sample no. 4, (0.5mm), (a, b, c) XPL, and (d) PPL, showing extensive alteration of biotite and Fe-oxide stained fractures	42
4.5	Representative photomicrographs of sample no. 5, (0.5mm), XPL, showing prominent quartz and feldspar grains with lower amounts of alteration, thus having second highest (MPa) values for UCS and SRH	43
4.6	Representative photomicrographs of sample no. 6, (0.5mm), XPL, showing extensive biotite alteration and fractured quartz grains,	44

	thus having lower (MPa) values for UCS and SRH	
5.1	UCS (Mpa) vs SRH (Mpa) of Mansehra Granite	50
5.2	UCS (Mpa) vs Petrography (%) of Mansehra Granite	52
5.3	SRH (Mpa) vs Petrography (%) of Mansehra Granite	52
5.4	SRH (Mpa) vs UCS (Mpa) correlation of Mansehra Granite	54
5.5	SRH (Mpa) vs Petrography (%) correlation of Mansehra Granite	55
5.6	UCS (Mpa) vs Petrography (%) correlation of Mansehra Granite	56

LIST OF ABBREVEATIONS

UCS	-	Uniaxial Compressive Strength
		or
		Unconfined Compressive Strength
SRH	-	Schmidt Rebound Hammer
ISRM	-	Internal Society for Rock Mechanics
IAEG	-	International Association of Engineering Geology and Environment
IS	-	Indian Standard
GS	-	Geological Society Engineering Group Working Party
ASTM	-	American Standard for Testing and Materials

CHAPTER 1

INTRODUCTION

1.1 Background

Engineering geology is an interdisciplinary subject that uses geological information for the planning, design, construction and maintenance of civil and mining engineering works. It is about the understanding of the behavior of earth materials such as rocks and soils when applied stresses are applied by engineering works. The ability and safety of any project constructed on, in or using rock depends most critically on rock strength. As Goodman (1989) points out, rock mechanics is the most interdisciplinary of all subjects with uses that range from geology to geophysics, from mining to petroleum, and from civil engineering to all other applications. The strength parameters of the rock mass are also critical to the design of the dam, the methods of construction, and the stability of the structure, whether the engineer is involved in the design of a dam abutment, the design of a highway cutting, or the design of a tunnel in a mountain range.

The importance of engineering geology has grown in proportion to the scale and complexity of modern infrastructure. Urbanization in the mountainous and geologically active terrains like the Himalayas or the Andes, demand rigorous characterization of subsurface materials. Bell (2007) emphasizes that the main aim of engineering geology is to ensure that geological factors affecting the location, design, construction, operation,

and maintenance of engineering works are recognized and adequately mitigated. Without an understanding of rock and soil mechanics, costly failures such as slope collapses, tunnel roof failures, and foundation failures can occur.

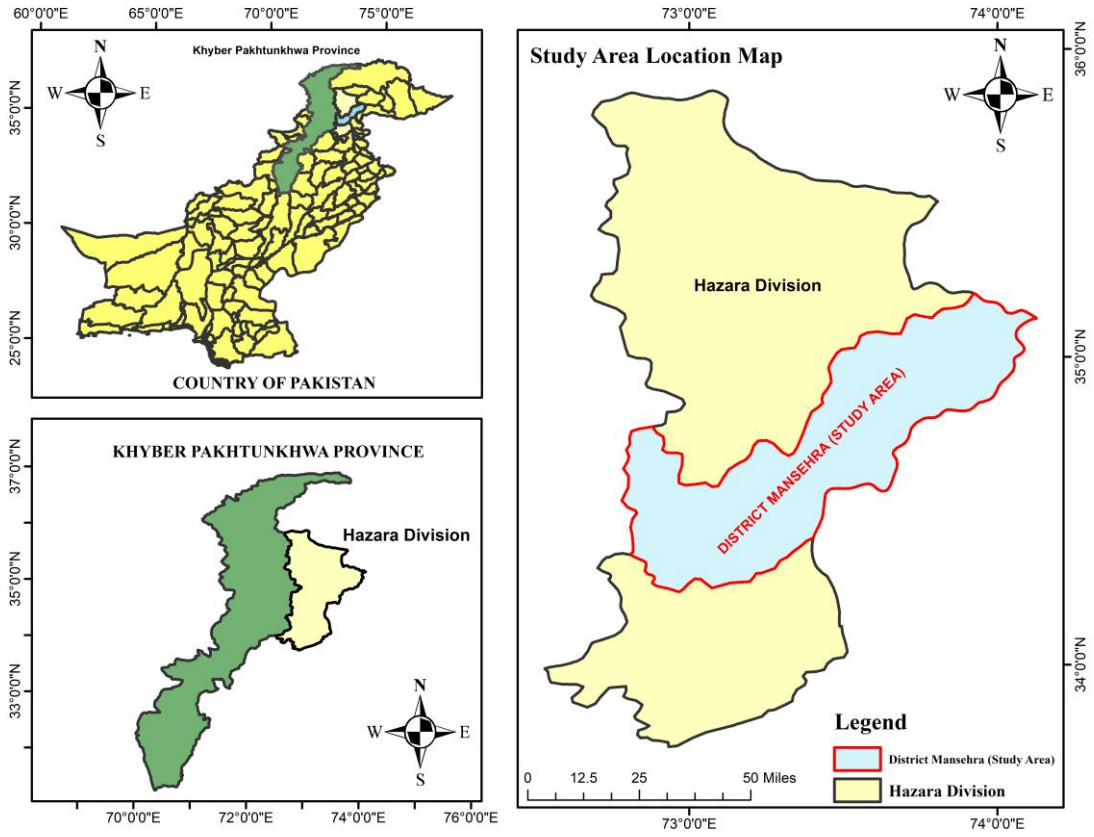


Figure 1.1 Location map of the study area showing District Mansehra (highlighted in blue color and marked by red) from where sampling was done, Khyber Pakhtunkhwa, Pakistan (ArcMap 10.5)

1.2 Rock and soil mechanics

Rock mechanics deals with the mechanical properties of rocks and how to apply this information to engineering problems involving rock materials (Goodman, 1989). The discipline distinguishes between the intact rock material which is deemed a continuous body of rock as tested in the laboratory, and the rock mass, which includes the intact material together with all the discontinuities such as joints, faults, bedding planes, and fissures (Hudson & Harrison, 1997). This distinction is important because the strength of a rock mass is almost always significantly lower than that of the corresponding intact specimen, owing its lower strength to its weakening effect from structural discontinuities.

Soil mechanics deals with the behavior of nonaggregate or weakly bonded earth materials. Terzaghi (1943) laid the foundations of modern soil mechanics by formulating the principle of effective stress, which dictates that the mechanical behavior of a saturated soil is governed not by the total stress acting on it, but rather by the effective stress which is the difference between total stress and pore water pressure. Rock and soil mechanics are often treated as separate sub fields of engineering geology, they still share the same theoretical framework of mechanics and highly overlap with regards to the study of weak rocks, residual soils, and weathered rock masses (Bell, 2007).

1.2.1 Rock strength and its measurement

Rock strength is the maximum stress the rock can withstand before complete failure. The most common is the uniaxial compressive strength (UCS) of a cylindrical specimen loaded along its axis until failure. UCS is easily measured and is a basic index property for engineering classification. The International Society for Rock Mechanics

(ISRM) has established a set of testing procedures that ensures uniformity and consistency in testing results among laboratories throughout the world (Brown, 1981).

In addition to uniaxial compression, the triaxial compressive test provides confining pressure to the specimen that provides a more realistic simulation of in situ stresses. For soils and rocks, the Mohr Coulomb failure criterion is still widely accepted and defines shear strength as a linear function of normal stress, controlled by cohesion and internal friction angle, respectively (Goodman, 1989). The non-linear Hoek-Brown failure criterion is now widely accepted for rock masses. This empirical criterion was developed by Hoek and Brown (1980) for jointed rock masses and is based on the uniaxial compressive strength of the intact rock, two material constants (m and s), which depend on the type of rock and the quality of the rock mass, respectively. The criterion has been modified and improved several times (Hoek et al., 2002), most significantly by incorporating the Geological Strength Index (GSI) which offers a geologically intuitive means of estimating rock mass properties from field observations (Marinos & Hoek, 2000). Indirect methods of strength estimation are also important in engineering geology. The point load strength index (Is50) offers a rapid field or laboratory based estimate of UCS through a simple empirical conversion factor (Broch & Franklin, 1972). The Schmidt rebound hammer test provides a nondestructive in situ measure that correlates with UCS and is especially useful for quick assessments of rock exposures (Aydin & Basu, 2005). These indirect techniques are particularly valuable during preliminary investigations when large numbers of test results are needed and time and resources are limited.

1.2.2 Factors controlling rock strength

Rock strength is controlled by a combination of factors including; mineral composition, texture, porosity, degree of weathering, the nature and density of

discontinuities found therein. Quartz rich rocks such as quartzites and granites tend to exhibit higher compressive strengths, than rocks dominated by phyllosilicates like mica and chlorite. Grain size plays an important role; fine grained rocks are generally stronger than their coarse grained counterparts because smaller grains present fewer crack paths (Tugrul & Zarif, 1999). Porosity is inversely related to strength; highly porous rocks such as sandstones and tuffs are markedly weaker than dense, low porosity igneous rocks (Bell, 2007). Moisture content can reduce rock strength. Colback and Wiid (1965) demonstrated that the uniaxial compressive strength of saturated quartzite shale can be as low as half that of the same material when tested dry, a phenomenon attributed to the reduction in molecular cohesive strength at grain boundaries in the presence of moisture. This sensitivity to moisture content is highly emphasized on the importance of groundwater characterization and modelling in engineering geology.

1.2.3 Rock mass classification systems

Because intact rock properties alone are insufficient to characterize the engineering behavior of a rock mass, several classification systems have been developed to integrate intact strength with discontinuity characteristics. Bieniawski's Rock Mass Rating (RMR) system uses six parameters including; UCS, Rock Quality Designation (RQD), discontinuity spacing, discontinuity condition, groundwater, and orientation of discontinuities which are used to assign a numerical rating that predicts rock mass behavior and guides support design (Bieniawski, 1989). Barton's Q-system (Barton et al., 1974) provides an alternative classification based on six different parameters including; block size, inter block shear strength, and active stress. Both systems have been extensively validated through decades of application in tunnelling, mining, and slope engineering projects worldwide since their inception.

1.3 Importance of engineering geology

The importance of engineering geology in protecting human life, infrastructure and the environment is illustrated by the catastrophic events that occurred at the Vajont Dam in 1963, for which insufficient geological investigation took place before a large landslide killed over 2,000 people (Jaeger, 1972). Systematic site investigation can identify potential hazards such as slope instability, seismicity, adverse groundwater conditions and swelling ground before the construction works commence, and early rock strength and deformability characterization can optimize design, select appropriate excavation methods, and minimize the risk of cost overruns (Bell, 2007) which is the most common failing in civil engineering projects due to poor site investigation. In tunnelling, the New Austrian Tunnelling Method (NATM) uses continuous monitoring of rock mass and adaptive support design based on rock mass classification systems like RMR and the Q system (Bieniawski, 1989); in dam construction, the Hoek–Brown criterion and Mohr–Coulomb parameters are used to assess foundation stability along discontinuities, taking into account the orientation, persistence, roughness, and infilling of the discontinuities (Hoek et al., 2002); and in slope analysis, stereographic projection and limit equilibrium methods are used to evaluate the orientation, persistence, roughness, and infilling of the discontinuities (Goodman, 1989). Engineering geology is also a major component of environmental management in relation to contaminant pathway prediction and radioactive waste disposal siting (Hudson & Harrison, 1997); adequate bearing capacity of surface structures is provided by point load tests and Schmidt hammer surveys (Aydin & Basu, 2005); rocks are used as raw materials such as aggregate, riprap and railway ballast, and their suitability is determined by their mineralogical and geotechnical properties (Bell, 2007).

1.4 Significance of the study

The study is of great scientific and practical importance for the understanding of the Mansehra Granitic Complex and its engineering behavior. It has provided baseline geotechnical and petrographic data for six representative granite samples, and a foundational geotechnical and petrographic dataset for the rock mass of the Hazara Basin to guide future investigations, geohazard assessments, and infrastructure projects in the area. Moreover, the study relates quantitatively the petrographic composition of granite to its mechanical behavior in terms of modal mineralogy (which is derived from thin sections) and measured engineering strength parameters, namely Uniaxial Compressive Strength and Schmidt Rebound Hardness, which helps in the understanding of how mineral scale properties may control the quality of rock mass in granitic terrains of northern Pakistan.

1.5 Literature review

Research on the petrographic and geotechnical characteristics of granitic rocks in northern Pakistan has developed gradually to establish a sound basis for engineering evaluation. Streckeisen's (1976) QAPF modal classification provided the basic petrographic framework for plutonic rocks, while Hawkins (1998) showed that the mechanical strength of granites is not an intrinsic property, but is determined by the quartz content, alteration, and microstructural features including microcracks.

In northern Pakistan, Sajid and Arif (2015) found that the strength values of Utla Granites were strongly correlated with the modal mineralogy, uniform grain size, and low porosity, hence, they suggested the petrographic characterization as a reliable predictive tool for engineering classification. Sajid et al. (2016) also showed that the strength of granites decreases steadily with heat treatment due to the formation of microcracks in

grain boundaries and cleavage planes. Anees et al. (2016) further emphasized the importance of modal mineralogy, by demonstrating that mineral proportions also govern natural radioactivity and gamma dose rates, with quartz, microcline, plagioclase, and biotite being the main minerals in a porphyritic fabric.

The emplacement ages derived by Naeem et al. (2016) (478 Ma, 475 Ma, 466 Ma) and the S-type, calc-alkaline, peraluminous character of the MGC, resulting from an Andean-type accretional orogeny, provide the tectonic context for the mineralogical and textural variations observed within the complex. This was confirmed by comparative field petrography and geochemistry by Sajid et al. (2018), who established megacrystic, highly peraluminous, calc-alkaline affinities with enrichment of LREE and negative Eu anomalies due to fractionation of feldspar. Zafar et al. (2019) recognized psammitic restites and quartzite xenoliths in the granite which are evidence of S-type crustal melting of Tanawal Formation metasediments, thus indicating a mineralogical and fabric variation within the granite that has direct implications for geotechnical variation across the complex.

Geotechnical testing of samples from the MGC and the surrounding lithologies by Naeem et al. (2015) indicated that the massive Mansehra Granite conformed to ASTM and BS requirements for dimension stone, road, and concrete aggregate, with mean UCS of ~62–66 MPa, and alkali silica reactivity was identified as a result of strained quartz, but the gneissic variety was found to be less appropriate for high specification applications. Khan et al. (2023) showed very good correlation between joint density, modal mineralogy and engineering performance in granitoids of the Karora Hydropower Project in Besham, offering an integrated structural-mechanical methodology directly transferable to systematic evaluation of the Mansehra Granite as a construction resource.

1.5.1 Research gap

Although the Mansehra Granitic Complex has been extensively studied geo-chronologically and geochemically, there are limited studies correlating the modal mineralogy with geotechnical parameters. There has been limited petrographic or mechanical integration in the geotechnical indices reported, and Schmidt Rebound Hammer testing has not been used in conjunction with Uniaxial Compressive Strength test for research work. This limited baseline integrated petrographic and geotechnical dataset is a significant knowledge gap in a region of rapid development of infrastructure in the tectonically active Himalayan foreland, which the present study aims to address.

1.6 Research Question(s)

1.6.1 Objectives

a) Petrographic analysis and determination of key geotechnical properties (UCS, and Schmidt Rebound Hammer) of Mansehra Granite.

b) Correlation between petrography and geotechnical properties of Mansehra Granite.

CHAPTER 2

GEOLOGY AND TECTONICS

2.1 Regional Geology

The Hazara Basin is a significant area in the northwestern Lesser Himalaya region of Pakistan between the Indian Plate and the Kohistan Island Arc in the western Himalayan fold and thrust system. The basin is located in the modern day Khyber Pakhtunkhwa province, and includes portions of the Hazara, Mansehra, Abbottabad, and Haripur districts, with a geologic history dating back to the late Precambrian (Neoproterozoic) to the Quaternary, a period of more than a billion years. To the north the Hazara Basin is bordered by the Main Mantle Thrust (MMT) which marks the suture between the Indian Plate and the Kohistan Arc; to the south and southeast it is bounded by the Main Boundary Thrust (MBT) and the Hazara Kashmir Syntaxis (HKS), one of the most prominent tectonic variations in the Himalayan chain (Bossart et al., 1988; Calkins et al., 1975).

The basin is a focus of geological interest for several reasons. It is one of the most complete stratigraphic successions in Pakistan ranging from Precambrian metasedimentary basement to Paleozoic platform carbonates to Mesozoic to Cenozoic shelf to molasse sequences. It is also a place of considerable mineralization including phosphate, ironstone, manganese and coal (Umar et al., 2015). The Mansehra Granitic Complex (MGC) is one of the largest and best documented Early Paleozoic plutons of the

entire Himalayan chain in the basin. The magmatic history of the northern margin of Gondwana from Cambro to Ordovician is documented in the MGC (Le Fort et al., 1986; Naeem et al., 2016).

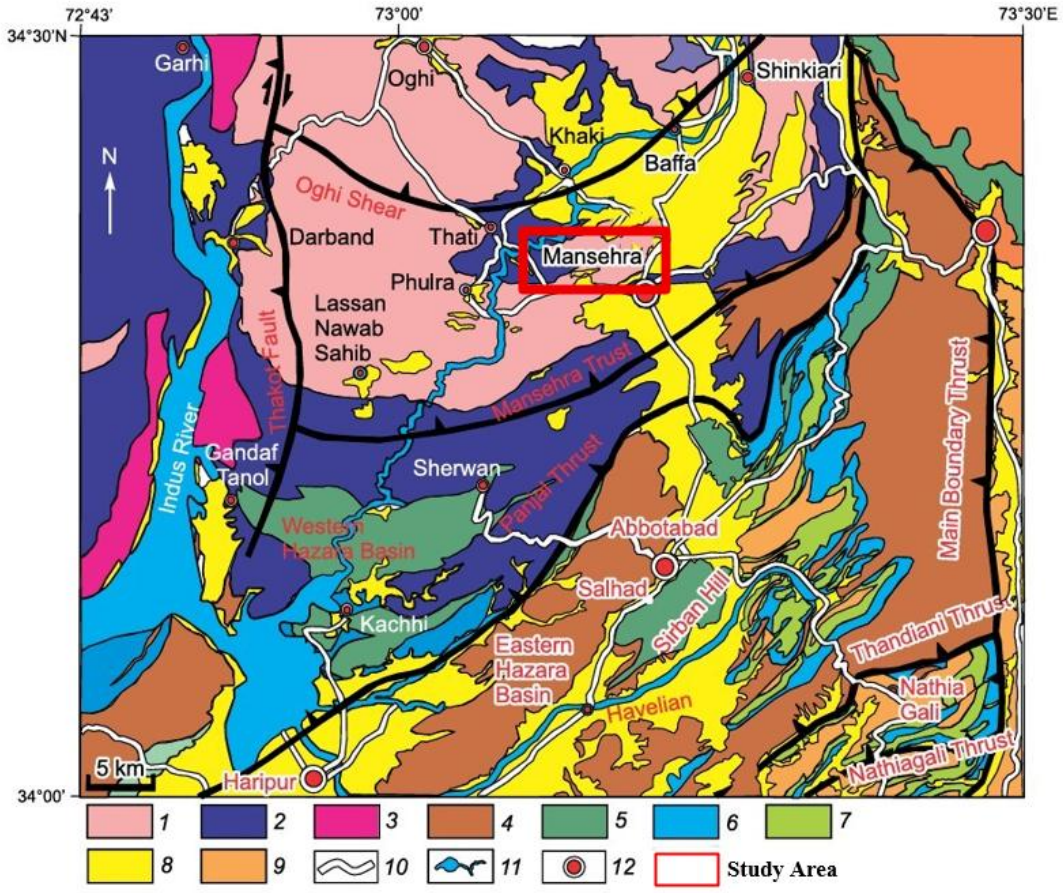


Figure 2.1 A geological map of the Hazara Basin depicting the spatial distribution of key rock units and geographic features, including; (1) Cambrian–Ordovician Mansehra Granite, (2) Meso-Neoproterozoic Tanawal Formation, (3) Paleoproterozoic Metamorphic Rocks, (4) Mesoproterozoic Hazara Formation, (5) Neoproterozoic–Cambrian sequences, (6) Jurassic; (7) Cretaceous, (8) Quaternary, (9) Paleogene, (10) Roads, (11) Rivers and Reservoirs, (12) Cities, Towns, and Villages, and the red box highlights the Study Area (after Iqbal et al., 2026)

2.2 Structural framework

According to DiPietro and Pogue (2004), the Hazara Basin is situated between the Hazara Kashmir Syntaxis (HKS) and the Indus Syntaxis, in the Lesser Himalayan tectonic zone of the Indian Plate. It is part of a classic fold and thrust belt located in the western Himalaya of Pakistan, flanked by the Salt Range Thrust and the Main Boundary Thrust (MBT) in the foreland and the Main Mantle Thrust (MMT), the extension of Indus-Tsangpo Suture Zone (ITZ) in the hinterland (DiPietro et al., 2021). The MMT separates the Indian Plate from the Kohistan Island Arc. The rocks also show evidence of deformation and metamorphism related to older events such as Neoproterozoic Gondwana rifting and Cambro-Ordovician orogenesis, the latter being responsible for the Mansehra Granitic Complex (Le Fort et al., 1986; Naeem et al., 2016). The dominant structural feature in the region is the tight antiformal loop of the HKS, which bends the MBT and Panjal Thrust from NW–SE to NE–SW trends (Bossart et al., 1988). It is also a major seismic center, responsible for the 2005 Kashmir earthquake (Mw 7.6) along the Balakot-Bagh Fault (Tahirkheli, 2011). Key thrust faults from north to south include the MMT, Panjal Thrust (PT), Nathia Gali Thrust, Hazara Thrust, and MBT (Bossart et al., 1988; Calkins et al., 1975). The western extension of the Main Central Thrust is interpreted to carry high-grade metamorphic rocks and separate the Higher Himalayan crystalline sequence from Lesser Himalayan metasediments (DiPietro & Pogue, 2004); the MBT is interpreted as the boundary with Cenozoic molasse (Murree and Siwalik formations). Thrusting migrated southward over time; the PT (14–9 Ma) in the Nathia Gali and the MBT (30–18 Ma). The western Hazara Ranges are further subdivided into three structural domains: Sherwan, Aluli and Pind Khan Khel, each having major synclines with Cambrian Abbottabad Formation cores and Precambrian Tanawal Formation limbs (Qasim et al., 2015).

2.3 Stratigraphy of the Hazara Basin

The stratigraphy of the Hazara Basin spans from the Neoproterozoic to the Quaternary, reflecting successive phases of sedimentation, magmatism, and tectonism on the northern margin of the Indian Plate. The oldest exposed units are the Neoproterozoic Hazara Formation (slate, phyllite, and greywacke) and the coeval Tanawal Formation (quartzite and quartz-mica schist), together forming the Precambrian metasedimentary basement of the Lesser Himalayan sequence (Calkins et al., 1975; Umar et al., 2015). Overlain by the Early Cambrian Abbottabad Formation, a shallow marine succession of dolomite, cherty limestone, and quartzite sandstone (Qasim et al., 2014; Umar et al., 2015). The Ordovician is represented by the emplacement of the Mansehra Granitic Complex (483–466 Ma), a peraluminous S type pluton generated by crustal melting of the Tanawal Formation, (Naeem et al., 2016; Ogasawara et al., 2019). The Permian Panjal Volcanic Group records continental flood basalt emplacement during NeoTethys rifting (DiPietro & Pogue, 2004; Bossart et al., 1988). The Mesozoic succession comprises of Triassic limestones, the Jurassic Samana Suk Formation, and the Cretaceous Chichali, Lumshiwal, and Kawagarh Formations, reflecting progressive deepening as the Indian Plate advanced northward (Calkins et al., 1975; Umar et al., 2015). The Paleogene records marine to syn collisional deposition through the Hangu Formation, Lockhart Limestone, Patala Shale, Margalla Hill Limestone, Chorgali, and Kuldana Formations (Calkins et al., 1975; Umar et al., 2015). The sequence is capped by the Neogene Murree Formation, the Siwalik Group, and Quaternary alluvial and glacial deposits (Calkins et al., 1975).

Table 2.1 Generalized Stratigraphy of Mansehra region, the table shows formations from the Precambrian to recent with the formation of interest highlighted in green (Awan et al., 2021)

Formation	Age	Description
Alluvium	Recent	Unconsolidated deposits of gravel, clay, and pebbles, etc
Siwaliks Group	Miocene to Pliocene	Sandstone, siltstone, clays, and conglomerates
Murree Formation	Early Miocene	Cyclic order of sandstone and shale with subordinate claystone and conglomerates
Kuldana Formation	Middle to Late Eocene	Siltstone and fine-grained sandstone
Chorgali Formation	Early Eocene	Siltstone and dolomitic limestone, calcareous shale
Margala Hill Limestone	Early Eocene	Limestone with subordinate greenish-grey shale
Patala Formation	Late Paleocene	Khaki shale and marl with subordinate sandstone and limestone
Lockhart Limestone	Early Paleocene	Massive, hard, and thick-bedded grey to medium grey nodular and flaggy limestone

Hangu Formation	Early Paleocene	Sandstone, laterite, bauxite, fireclay, and coal
Unconformity		
Mansehra Granite	Cambrian to Ordovician	Quartz alkali feldspar and sodium-rich plagioclase and accessory minerals are micas (muscovite and biotite). Xenolith present in some places.
Abbottabad Formation	Cambrian	Chiefly dolomite, limestone, chert bands, and black shale
Tanol Formation	Precambrian	Metasediments, phyllite, and quartzite schist
Hazara Formation	Precambrian	Slates with subordinate metasediments.

2.3.1 The Mansehra Granitic Complex

The MGC is the largest intrusive body in the Hazara Basin, and one of the most important plutonic suites in the Lesser Himalayan belt, exposed throughout Mansehra district, KPK (Calkins et al., 1975; Le Fort et al., 1980). It is located in the hanging wall of the Panjal Thrust and belongs to the Lesser Himalayan Granite Belt, a chain of early Paleozoic peraluminous granitoids that extend from Pakistan through India, Nepal, and into southern Tibet, which were formed during the Cambro-Ordovician orogenesis along

the northern margin of east Gondwana (Le Fort et al., 1983, 1986). The complex is characterized by the Mansehra Granite, Hakale Granite and subordinate leucogranitic, pegmatite and microgranite bodies intruding the Tanawal Formation with well-developed contact aureoles of andalusite hornfels, cordierite-bearing assemblages and migmatites (Naeem et al., 2021).

Petrographically, the Mansehra Granite is a medium to coarse grained porphyritic granite with abundant K-feldspar megacrysts (2-10 cm) and locally formed gneissic foliation due to Himalayan-age solid state deformation (Arif et al., 1999; Naeem et al., 2021). The Hakale Granite is a finer-grained, equigranular two-mica granite, and leucogranites are late-stage fractionation products (Naeem et al., 2021). The S-type anatectic origin is confirmed by psammitic and pelitic restites.

Geochemically, the MGC is strongly peraluminous with LREE enrichment, negative Eu, Nb, Sr and Ti anomalies, and elevated Rb and Cs, which are consistent with partial melting of metasedimentary sources (Naeem et al., 2021; Ogasawara et al., 2019). The Mansehra Granite formed via biotite dehydration melting of the Tanawal Formation at >5 kbar and >700°C, while the Hakale Granite formed at shallower depths through muscovite fluid-absent melting (Naeem et al., 2021). The high initial 87Sr/86Sr ratios (0.727-0.847) confirm a heterogeneous evolved crustal source (Le Fort et al., 1980; Naeem et al., 2021) and the presence of andalusite in the contact aureole suggests shallow emplacement at <~15 km depth (Naeem et al., 2021). U-Pb zircon geochronology (SHRIMP and LA-ICP-MS) has provided crystallization ages for the Mansehra Granite of 483–476 Ma, leucogranites of ~475 Ma, and the Hakale Granite of ~466 Ma, which firmly places the MGC in the Cambro-Ordovician and correlates it with the broader Lesser Himalayan granitic belt (Naeem et al., 2016; Ogasawara et al., 2019). Inherited zircon cores (889–664 Ma, 1862–1595 Ma, ~2029 Ma) indicate Precambrian Tanawal Formation protolith, with ancient crustal sources (Ogasawara et al., 2019). The petrographic, geochemical and isotopic data together support crustal melting of the

Tanawal metasediments during an Andean-type accretional orogeny along the Proto-Tethyan margin of east Gondwana (Naeem et al., 2016; Ogasawara et al., 2019).

CHAPTER 3

METHODOLOGY

3.1 Work methodology

For this study, fresh outcrops of Mansehra Granite were sampled at six representative locations throughout Mansehra city and its surrounding areas, with a particular emphasis on section along the roads. Weathering classification of the Geological Society Engineering Group Working Party (1977) was used to select the sampling localities and the classification was based on six grades of weathering from Grade I (fresh, no visible weathering) to Grade VI (residual soil). Only outcrops with material in Grade I to Grade II classification, characterized as fresh to slightly stained rock with no alteration of the mineral fabric was sampled and localities with advanced oxidation staining, development of clay minerals, or mechanical disaggregation of minerals of the feldspar and biotite grains were avoided. This criterion is also seen as consistent with the recommendations of ISRM (1978) that rock samples for mechanical testing should be taken from areas of intact unaltered rock with no pre-existing damage caused by surficial weathering processes. The surface of each accepted locality was thoroughly inspected with a geological hammer to remove any remaining weathered material from the rock surface to expose a fresh surface prior to sampling. The location of each sampling station was determined by using a hand-held GPS receiver for precise georeferencing and documentation of the spatial distribution of samples throughout the complex.

A representative bulk rock block of adequate size to produce a complete cylindrical core specimen was sampled from each of the six selected outcrops, avoiding planes of preexisting fractures, joints or foliation that would make the specimen mechanically non representative. The extracted blocks were wrapped individually, labeled with their field identification codes, and shipped to the lab following the preservation and transport guidelines outlined in (ASTM D 5079), which states that core or block samples should be protected from mechanical damage, changes in moisture content, and extremes of temperature while in storage and transport. In the laboratory, each bulk block was core-drilled to obtain appropriate cylindrical core samples, which resulted in six suitable cores being obtained for the study, using a water-cooled core barrel. The drilling procedure was conducted in accordance with Standard Practice for Rock Core Drilling and Sampling of Rock for Site Exploration (ASTM D 2113-14) that addresses the specifications for equipment, orientation of drilling, fluid use, and recovery of cores from hard and soft rock. The core specimens were prepared and trimmed to meet the dimensional and shape tolerances specified in (ASTM D 4543-19), Standard Practices for Preparing Rock Core as Cylindrical Test Specimens, which called for a specimen length to diameter ratio of 2:1, flat end surfaces parallel to one another, and cylindrical surfaces free of irregularities.

Prior to mechanical testing, one of ends of each core specimen were chipped retained for petrographic thin section preparation in accordance with (ASTM C 295-08), the Standard Guide for Petrographic Examination of Aggregates for Concrete, which recommends petrographic analysis as a mandatory preliminary step before mechanical testing of rock specimens owing to the fundamental influence of mineralogical composition, grain size, texture, and alteration on engineering performance. These end offcuts, being freshly cut surfaces representative of the same material as the core, provided ideal material for thin section manufacture without consuming any portion of the core length needed for mechanical testing. The drilling of bulk samples for core extraction, thin section making along with UCS test was done at the engineering geology laboratory of Bahria School of Engineering and Applied Sciences Islamabad, Schmidt

Rebound Hammer Testing was done at Tunneling Institute of Pakistan and Petrography was done at the National Museum of Natural History, Islamabad.

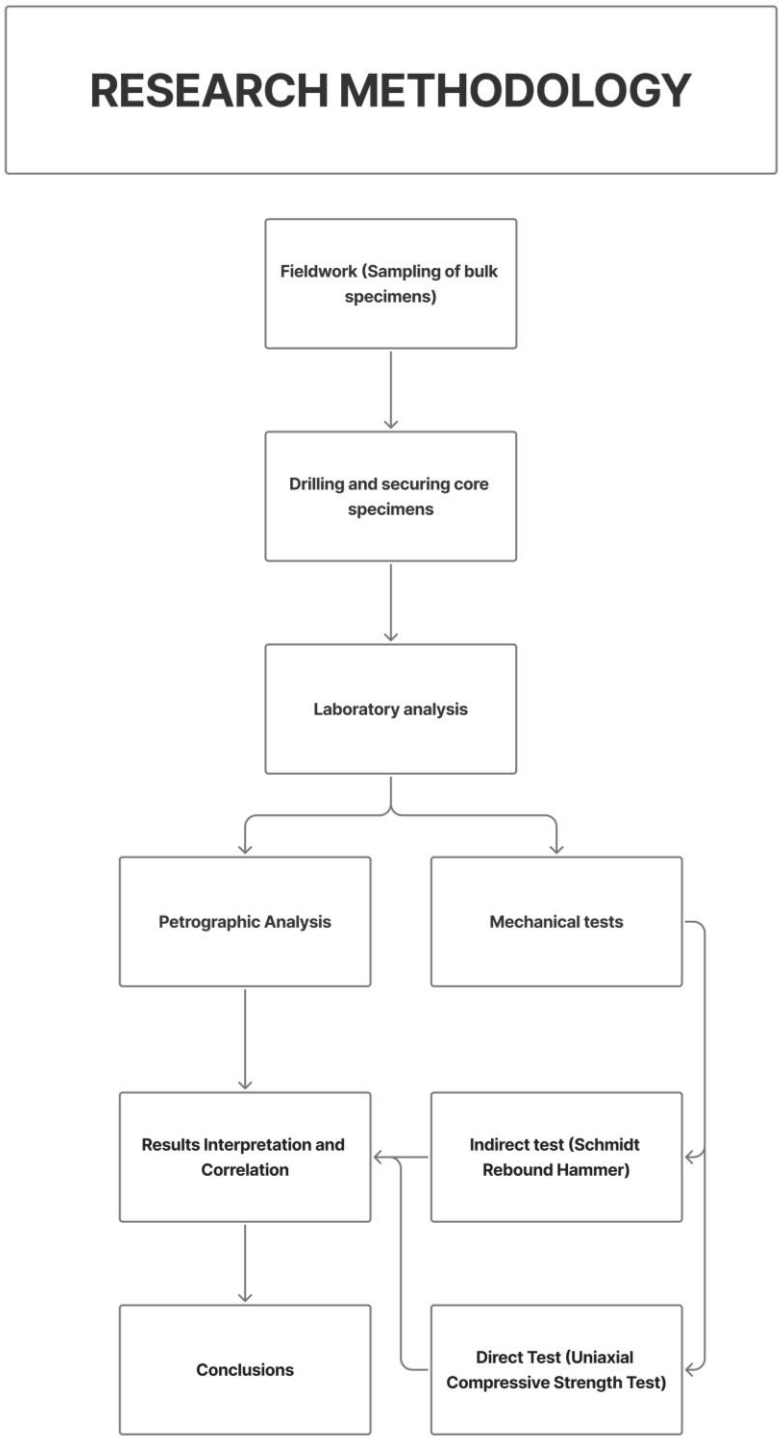


Figure 3.1 Adapted methodology for this study



Figure 3.2 Photograph of the bulk specimens taken during fieldwork of Mansehra Granite

Table 3.1 Coordinates of the Samples of Mansehra Granite

Sample	Latitude	Longitude
S1	34.35959	73.25771
S2	34.35988	73.25748
S3	34.46201	72.99325
S4	34.44347	72.93949
S5	34.44278	72.93929
S6	34.44436	72.94205

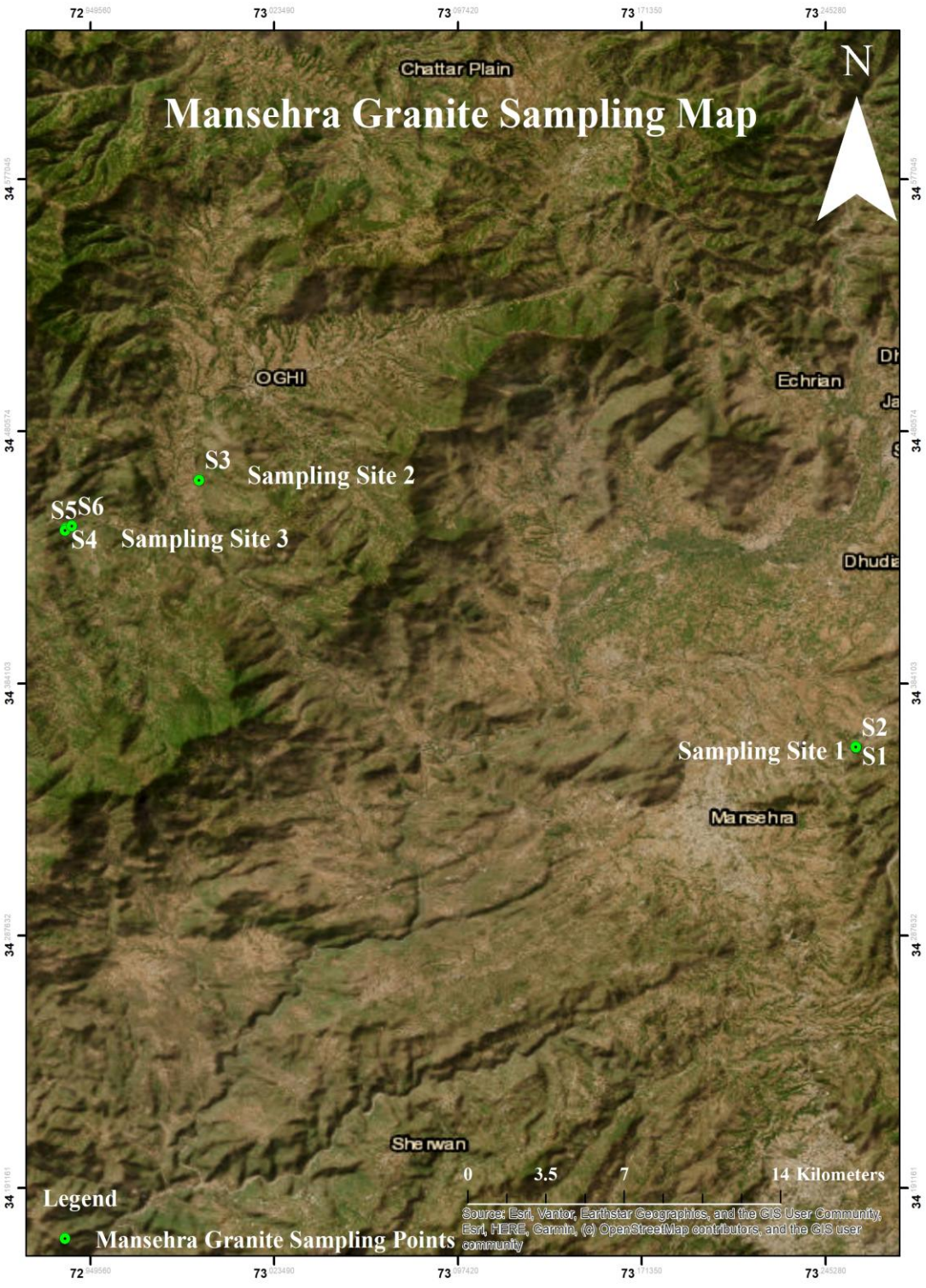


Figure 3.3 Bulk specimens sampling location map of Mansehra Granite (ArcMap 10.5)



Figure 3.4 Coring of bulk specimens of Mansehra Granite



Figure 3.5 Secured core specimens from bulk samples of Mansehra Granite

3.1.1 Thin section preparation

Thin sections for petrographic analysis are prepared from chips of cylindrical core specimens obtained during drilling. The preparation follows a sequential multi step protocol beginning with the initial lapping on an iron lap using 400-grit carborundum powder to produce a flat surface, followed by a finer finish on a glass plate with 600-grit carborundum. Once the lapped face is dried on a hot plate, it is permanently bonded to a clean glass slide using epoxy resin.

After the epoxy has fully cured, the bonded slab is sectioned close to the glass surface using a thin section saw and the remaining thickness is progressively reduced on a grinding machine. The section is then hand lapped on a glass plate with 600 grit carborundum until the standard petrographic thickness of 30 microns is achieved, with an optional pre-polish step using 1000 grit carborundum available for improved surface quality. In the final step, the thinned section is polished using a nylon cloth and diamond paste on a polishing machine until the surface is of sufficient optical quality for transmitted light microscopy.

The finished slide is inspected under the polarizing microscope, and if quality is found to be unsatisfactory at any stage, the relevant steps are repeated before the thin section is approved for formal petrographic analysis.



Figure 3.6 Slab preparation from core specimens at Bahria University Islamabad

3.1.2 Petrographic Analysis

Petrographic analysis of rock specimens is recommended by the American Society for Testing and Materials (ASTM C 295-08) owing to the fundamental influence that the mineralogical and textural characteristics of a rock exert on its engineering and mechanical properties. In granites, the mechanical behavior of intact rock is largely influenced by how the major rock forming minerals including; quartz, K-feldspar, plagioclase, biotite, and muscovite are proportioned, sized, and spatially distributed throughout the rock mass. Secondary alteration products further influence the rock masses, and together these factors shape how the rock behaves when stresses are applied. Before any mechanical testing can be done on intact rock specimens or aggregate materials, a well-defined set of preparatory steps must be ensured. Thin section preparation is a key part of this process, as it allows the rock specimens to be examined at

the microscopic scale where many of its most important characteristics can be studied in detail.

The examination is the second step and involves studying these thin sections under a polarizing microscope. During the study photomicrographs are typically taken along the way to capture features such as grain boundaries, mineral cleavage, foliation, alteration textures, and microfractures. Thus, petrographic analysis is not merely a formality but is fundamental to assessing whether a granitic rock is mechanically sound and suitable for use in civil and geotechnical applications. The observations which are made at this stage also provides a foundation for understanding the correlations that are made when petrographic data is later correlated with mechanical test results.



Figure 3.7 Polarized microscope at geoscience lab of National Museum of Natural History, Islamabad

Table 3.2 Generalized magnification scheme for objective lens

Objective Magnification	Numerical Aperture	Focal Length	Field of View	Use
4x	0.10	16mm	5mm	Scanning slide, low power overview
10x	0.25	4mm	2mm	Low power scanning and overview
40x	0.65	0.65mm	0.5mm	Medium power, cell structure
60x	0.80	0.4mm	0.3mm	Medium high power, fine cellular details
100x Oil	1.25	0.2mm	0.2mm	High power with oil, subcellular details
150x Oil	1.25	0.13mm	0.15mm	Very high power with oil, subcellular fine structure

3.1.3 Schmidt Rebound Hammer Test (Indirect-ASTM D 5873-00)

The Schmidt Rebound Hammer (SRH) test is a nondestructive method for estimating the surface hardness and indirect compressive strength of intact rock specimens, conducted in accordance with ASTM D 5873-00. Rock core specimens are prepared with smooth, clean surfaces and are tested either on the flat end face of the core or on the smoothed lateral surface, with the testing orientation fixed at a vertical angle of 90 degrees. Prior to commencing any testing, the instrument is calibrated against a

standard steel anvil with a preassigned Brinell hardness value of 5000 N/mm², ensuring accuracy and consistency of all subsequent readings.

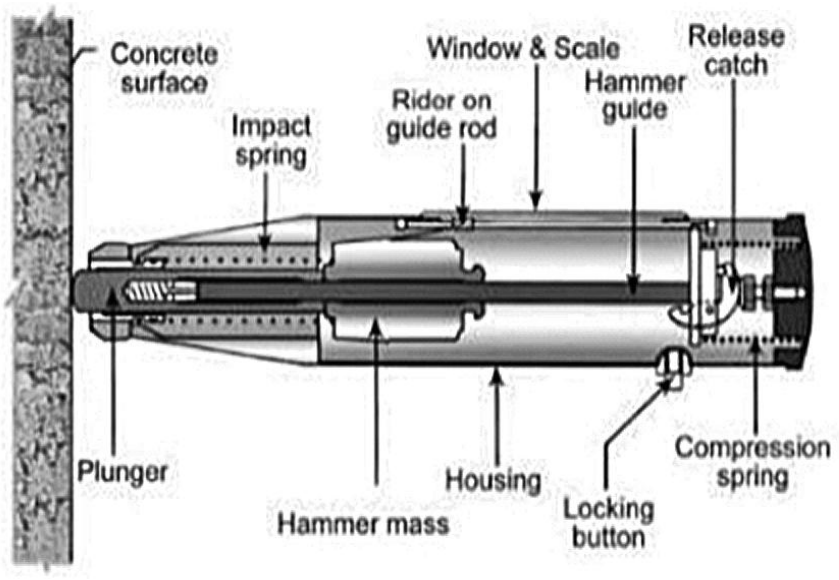


Figure 3.8 Generalized schematics of SRH

The operating principle of the instrument relies on a spring loaded plunger that delivers a fixed impact energy to the specimen surface that is typically 2.25 Nm for standard mass testing as prescribed by IS 13311 (Part 2): 1992 and the distance of rebound of the hammer mass is recorded as the rebound number. A weaker material absorbs more of the impact energy and returns a lower rebound value, while a harder and stronger material produces a correspondingly higher rebound number; strength estimates are then derived by correlating the averaged rebound values against standard reference charts.

Two readings are taken per specimen and averaged, and the result is classified against an established quality correlation scheme in which rebound numbers exceeding

40 indicate very good hard rock, values of 30 to 40 represent good quality material, 20 to 30 is classified as fair, and values below 20 denote poor material.

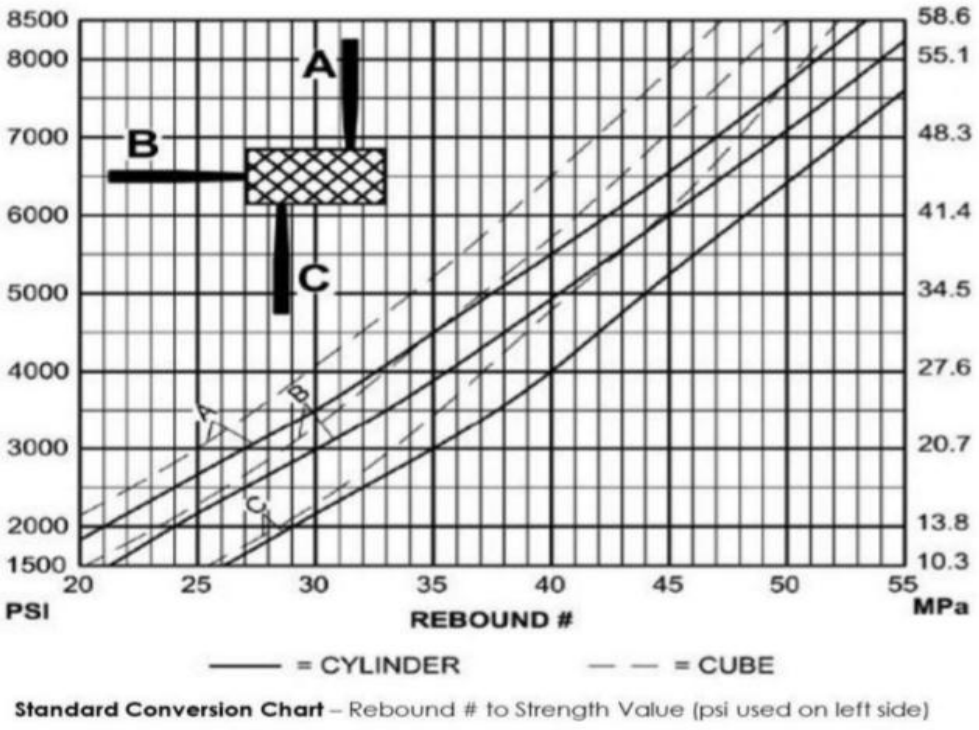


Figure 3.9 Graph for rebound value estimation

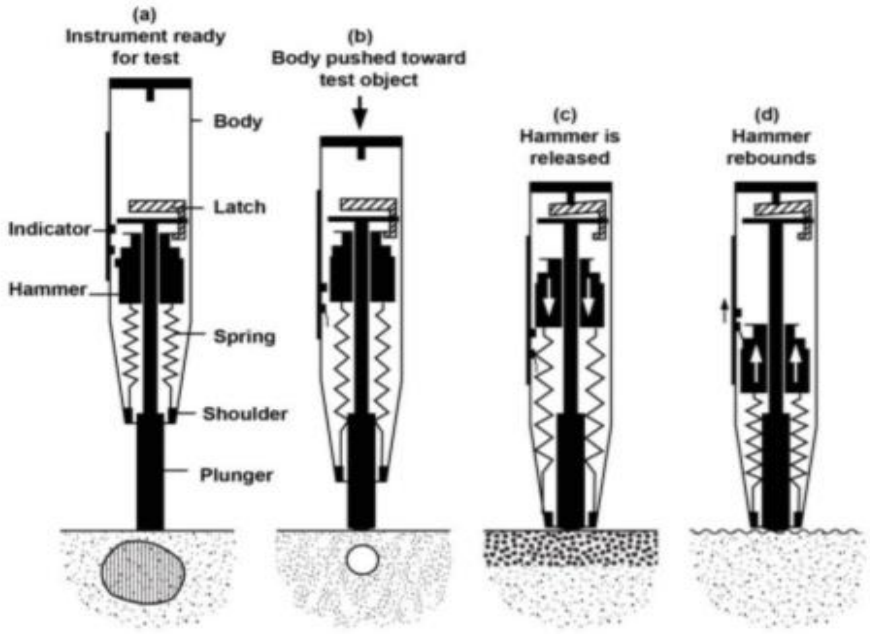


Figure 3.10 Generalized steps of SRH testing



Figure 3.11 Tunneling institute of Pakistan (Lab site where SRH tests were performed)

3.1.4 Uniaxial Compressive Strength Test (Direct-ASTM D 2938-95)

The Uniaxial Compressive Strength (UCS) test is a destructive procedure used to determine the uniaxial compressive strength of intact rock core specimens and is performed in accordance with ASTM D 2938-95. The test involves the axial loading of a cylindrical core specimen under no lateral confinement until failure, and the compressive strength is calculated using the formula from (ASTM D 2938-95) manual;

$$\text{Compressive Strength (qc)} = P/A$$

Where;

a) qc represents the peak axial stress at failure expressed as force per unit cross sectional area.

b) P = The maximum (failure) load applied to the rock specimen (in Newtons or Pounds force).

c) A = The cross-sectional area of the rock core specimen (in square millimeters or square inches).

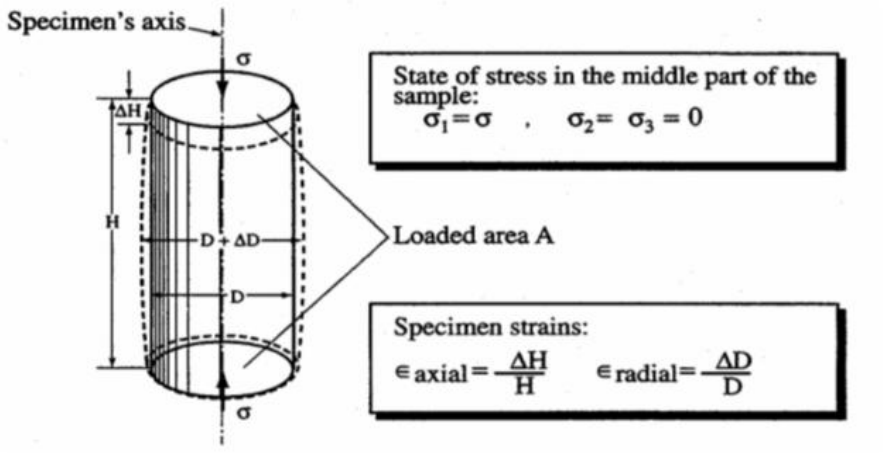


Figure 3.12 Cylindrical core specimen's definitions of stress conditions and strains (ASTM D 2938-95)

Specimens must conform to a cylindrical geometry with a length to diameter ratio of 2:1, with smooth, flat, and mutually parallel end faces cut perpendicular to the core axis as required by ASTM D 4543-19. While specimens of NX core diameter (44 mm) were conventionally used, the present study employs cores of 55 mm diameter with core lengths equal to twice the specimen diameter, both dimensions remaining within the acceptable range of the standard. The rate of axial loading applied to each specimen must remain within the limits prescribed by the ASTM procedure, as deviations significantly affect the recorded results; similarly, moisture content is noted prior to testing given its well documented influence on rock strength.

The UCS test remains the most direct and reliable means of characterizing rock compressive strength, and the values obtained are classified against internationally recognized grading schemes established by the Geological Society (1977), the International Association for Engineering Geology and the Environment (1977), and the International Society for Rock Mechanics (1981).



Figure 3.13 Performing UCS test on core 1 of Mansehra Granite



Figure 3.14 Performing UCS test on core 5 of Mansehra Granite



Figure 3.15 Performing UCS test on core 6 of Mansehra Granite

CHAPTER 4

RESULTS AND INTERPRETATION

4.1 Mechanical test results

The following results of SRH and UCS mechanical tests were obtained from the laboratory.

4.1.1 Uniaxial Compressive Strength (UCS)

The Uniaxial Compressive Strength (UCS) test was conducted on six Mansehra Granite specimens in accordance with ASTM D 2938-95, with the results of peak load and corresponding uniaxial compressive strength presented in Table 4.1. The peak loads recorded at failure range from a minimum of 294.60 kN for specimen S2 to a maximum of 356.37 kN for specimen S1, while the corresponding UCS values range from a minimum of 124 MPa recorded for S2 to a maximum of 150 MPa recorded for S1.

Among the remaining four specimens, S3 recorded a peak load of 301.70 kN with a UCS of 127 MPa, S6 recorded a peak load of 313.60 kN with a UCS of 132 MPa, S4 recorded a peak load of 327.80 kN with a UCS of 138 MPa, and S5 recorded a peak load of 344.50 kN with a UCS of 145 MPa.

The observed range within the dataset is 61.77 kN in peak load and 26 MPa in UCS, which represents consistent range of range across all six specimens. Mean peak load across the six specimens is 323.1 kN, and the mean Uniaxial Compressive Strength value is at 136 MPa.

Table 4.1 Results of uniaxial compressive strength test of Mansehra Granite

Sample No.	Peak Load (kN)	UCS (MPa)
S1	356.37	150
S2	294.60	124
S3	301.70	127
S4	327.80	138
S5	344.50	145
S6	313.60	132

4.1.2 Schmidt Rebound Hammer (SRH)

The Schmidt Rebound Hammer (SRH) test was conducted at Tunneling Institute Pakistan (TIP) on six sample specimens, with the results presented in Table 4.2. The average rebound values range from a minimum of 42.3 recorded for sample S2 to a maximum of 53.0 jointly recorded by samples S1 and S5.

The mean average SRH rebound value for all of the six samples is 48.3, and the mean strength value recorded is 63.1 MPa. None of the samples gave an SRH rebound

value below 40, which confirms that all the tested samples are mechanically competent and free of major surficial weathering or internal discontinuities that would otherwise suppress rebound response and give less observed values.

Table 4.2 Schmidt rebound hammer test results of Mansehra Granite

Sample No.	Avg. Rebound Value	Strength (MPa)
S1	53.0	71
S2	42.3	52
S3	44.2	56
S4	50.5	66.8
S5	53.0	71
S6	46.6	62

4.2 Petrographic analysis

Thin sections prepared from all six specimens of the Mansehra Granite were examined under plane-polarized light (PPL) and cross-polarized light (XPL) in accordance with ASTM C295/C295M-19, Standard Guide for Petrographic Examination of Aggregates for Concrete.

It establishes a framework for the identification and classification of rock and mineral constituents and for the determination of physical and chemical properties observed by petrographic techniques which are relevant to the behavior of geological

materials. Four representative photomicrographs were visually estimated for modal mineralogy.

Quartz is the most abundant mineral and is present as anhedral to subhedral grains with characteristic grey to blue-grey interference colors in XPL and complete colorless in PPL. The grain boundaries are sutured and interlocked in all samples and undulatory extinction is seen in Samples S1, S3, S4 and S5 which indicates intracrystalline strain. The most intense birefringence expression in the dataset is in quartz of the Sample S6 Image 1, which shows a particularly strong blue cyan interference color. Quartz forms a continuous interlocking framework around the larger feldspar phenocrysts and mafic grains in all specimens.

There are two types of K-feldspar in the sample set. Orthoclase has first order orange to tan interference colors in XPL and two good cleavages, and microcline is characterized by the presence of a grid like twinning pattern in XPL. Sample S1 has abundant large K-feldspar phenocrysts that are typical of the porphyritic nature of the Mansehra Granitic Complex, and they are fresh and show little internal alteration. In Sample S3 and S5, large K-feldspar phenocrysts are seen as near extinction grey fields in XPL and are confirmed to be K-feldspar by the presence of Fe oxide precipitates aligned in two mutually orthogonal directions. A common alteration feature is sericitization of the interiors of K-feldspar grains (represented by fine-grained silky aggregates as opposed to the grain interior), found in Samples S2, S3, S4, and S6, which is an indication of prolonged interaction with the hydrothermal fluids.

The presence of fine parallel striation across grain interior in XPL is a useful distinguishing feature of plagioclase from quartz (which is free of such striation) and from K-feldspar (which has a characteristic grid-like pattern of twinning). Plagioclase is the most common phase of the feldspar group in Sample S4 and is present as large subhedral grains that are scattered throughout the matrix. Samples S2 and S6 have well-developed corroded grain boundaries, which are characteristic of post magmatic fluid

interaction. The sliver of plagioclase at the edge of the large microcline grain has a very bright blue interference color in Sample S1 Image 2.

Biotite is the main mafic mineral in all specimens and is characterized in PPL by strong brown pleochroism, perfect basal cleavage and in XPL by anomalous brownish to olive khaki interference colors. Biotite is found to be small, relatively fresh, isolated grains in Sample S1, with well-preserved cleavage. There is little Fe-oxide staining. Biotite is progressively altered in Samples S2, S3, S4, S5 and S6, with the release of the iron during alteration forming limonite and hematite along cleavage planes and invading neighboring quartz and feldspar grains. A large, Fe oxide-replaced mass of biotite is one of the most prominent textural features in Sample S2, Image 2 and Sample S2, Image 3, while a single large biotite grain with two distinct cleavage directions dominates the field of view of Sample S3, Image 3. The elongated grain of biotite displaying the characteristic anomalous olive khaki XPL interference colour is particularly well displayed in Sample S4 Image 2. The alteration of biotite is systematic, from S1 to S6, and directly related to the measured strength of the rocks in the sample set.

Black opaque minerals (mainly magnetite and ilmenite) are present in all the samples as completely non-transmitting opaque grains in both PPL and XPL. They are primarily confined to inclusions along biotite cleavage planes, or are concentrated at biotite grain boundaries. In the more altered specimens, opaque mineral clusters are concentrated within biotite alteration zones, which are a result of iron mobilization and redistribution during the hydrothermal overprinting.

The most geotechnically relevant textural features observed in the photomicrographs are microfractures that are coated with Fe oxide precipitates, which are found in all specimens. The PPL photomicrograph of Sample S1 shows red brown curvilinear cracks that cut across quartz grains, and fracture networks cutting K feldspar phenocrysts are especially well-developed in Samples S3 and S5. In more biotite rich samples, additional continuous planar discontinuities are created by the ideal basal

cleavage of biotite, which are widened as the chemical breakdown of biotite proceeds in Samples S2, S3, S4 and S6. Sericite and muscovite are the secondary minerals identified in minor amounts throughout the sample set. Overall, the Mansehra Granite is porphyritic and has coarse K-feldspar phenocrysts in a medium grained granular to hypidiomorphic granular groundmass composed of quartz and feldspar.

Below is the modal mineralogy of Mansehra Granite, and photomicrographs taken from the thin sections prepared from core specimens of that have been annotated with observations as shown in table 4.3., and figures (4.1., 4.2., 4.3., 4.4., 4.5., and 4.6.).

Table 4.3 Modal mineralogy of Mansehra Granite

Serial No.	Sample Label	Quartz %	K-Feldspar %	Plagioclase %	Biotite %	Opaques %
1	S1	55	29	4	4	8
2	S2	52	6	14	18	10
3	S3	61	3	13	14	9
4	S4	45	5	28	18	4
5	S5	66	3	12	12	7
6	S6	47	8	19	18	8

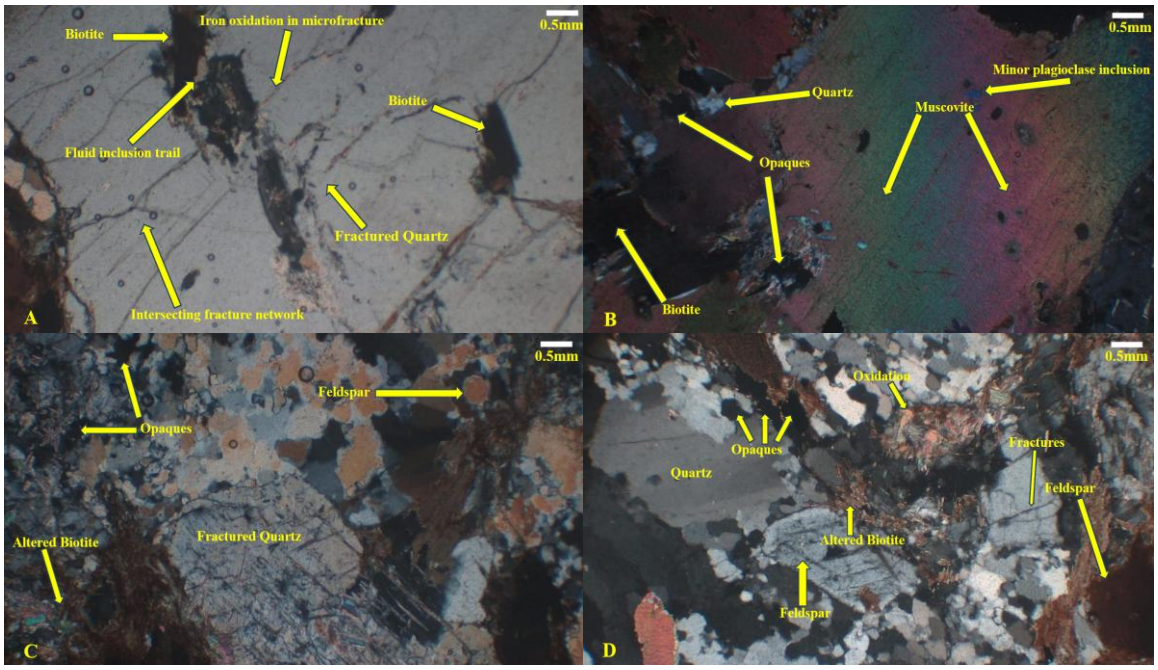


Figure 4.1 Representative photomicrographs of sample no. 1, (0.5mm), XPL, showing higher quartz and feldspar content with alteration of biotite and oxidation

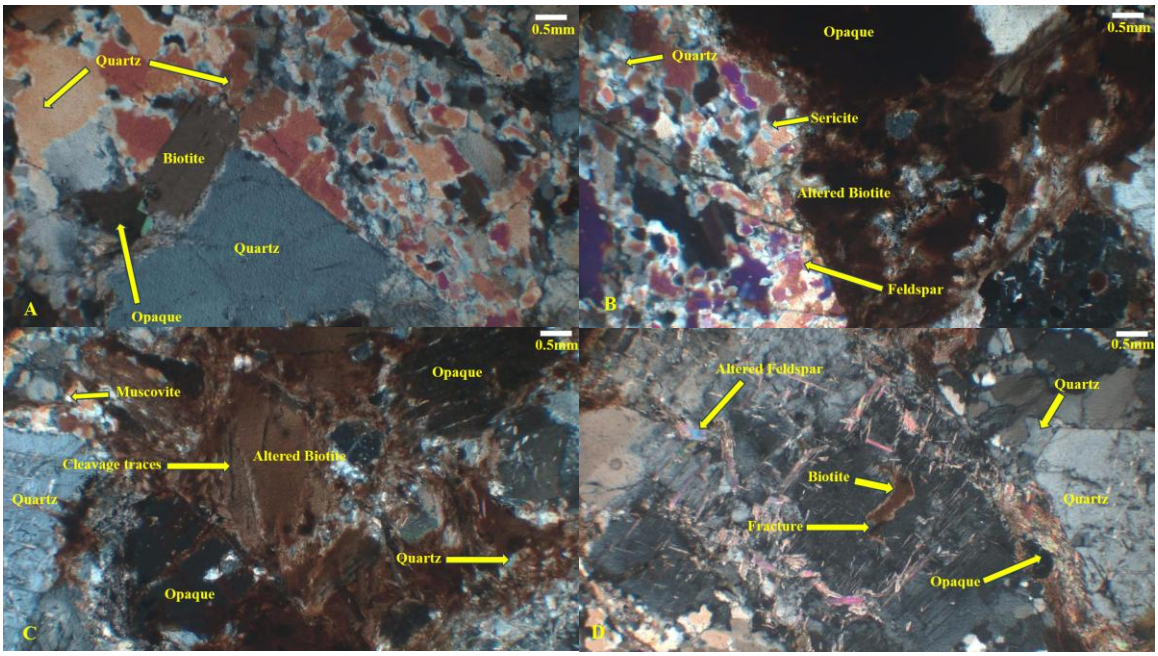


Figure 4.2 Representative photomicrographs of sample no. 2, 0.5mm, XPL, showing more prominent opaques and biotite alteration with cleavage traces which control mechanical anisotropy

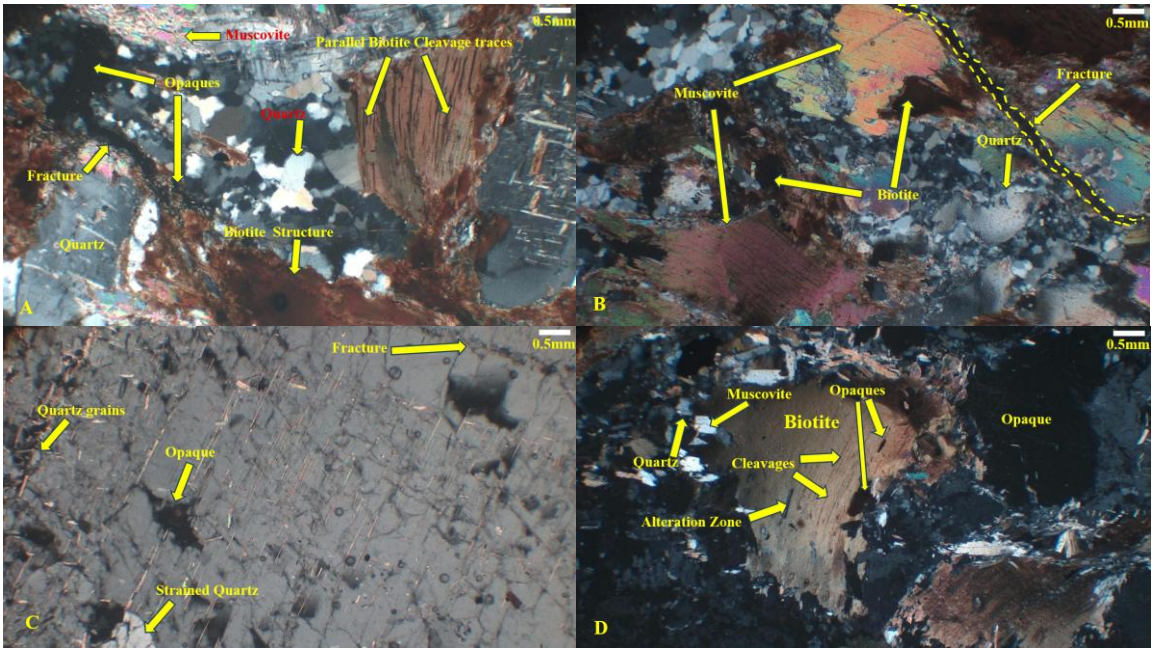


Figure 4.3 Representative photomicrographs of sample no. 3, 0.5mm, XPL, showing visible fractures, strained quartz grains, biotite grains with visible parallel cleavages, and extensive oxidation

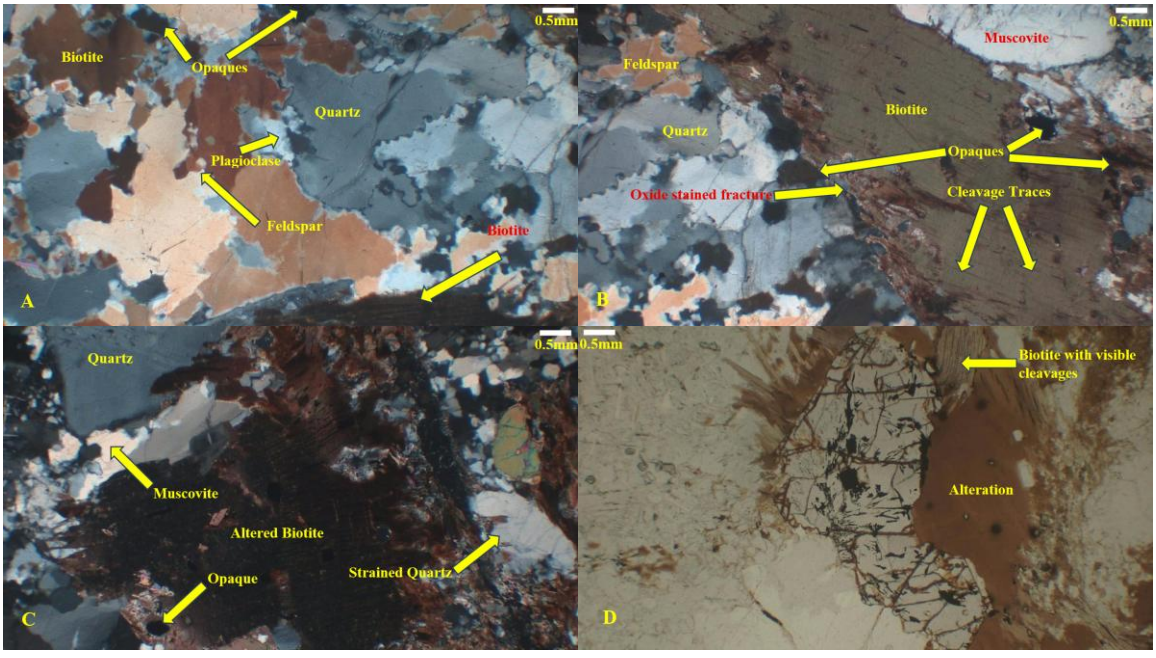


Figure 4.4 Representative photomicrographs of sample no. 4, (0.5mm), (a, b, c) XPL, and (d) PPL, showing extensive alteration of biotite and Fe-oxide stained fractures

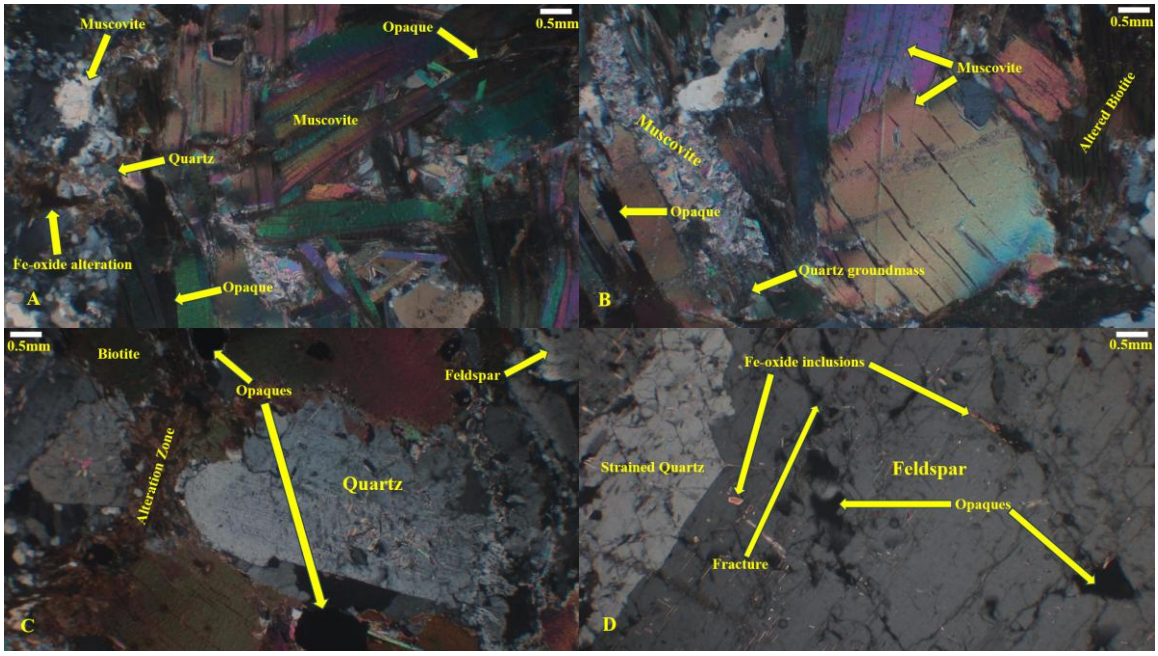


Figure 4.5 Representative photomicrographs of sample no. 5, (0.5mm), XPL, showing prominent quartz and feldspar grains with lower amounts of alteration, thus having second highest (MPa) values for UCS and SRH

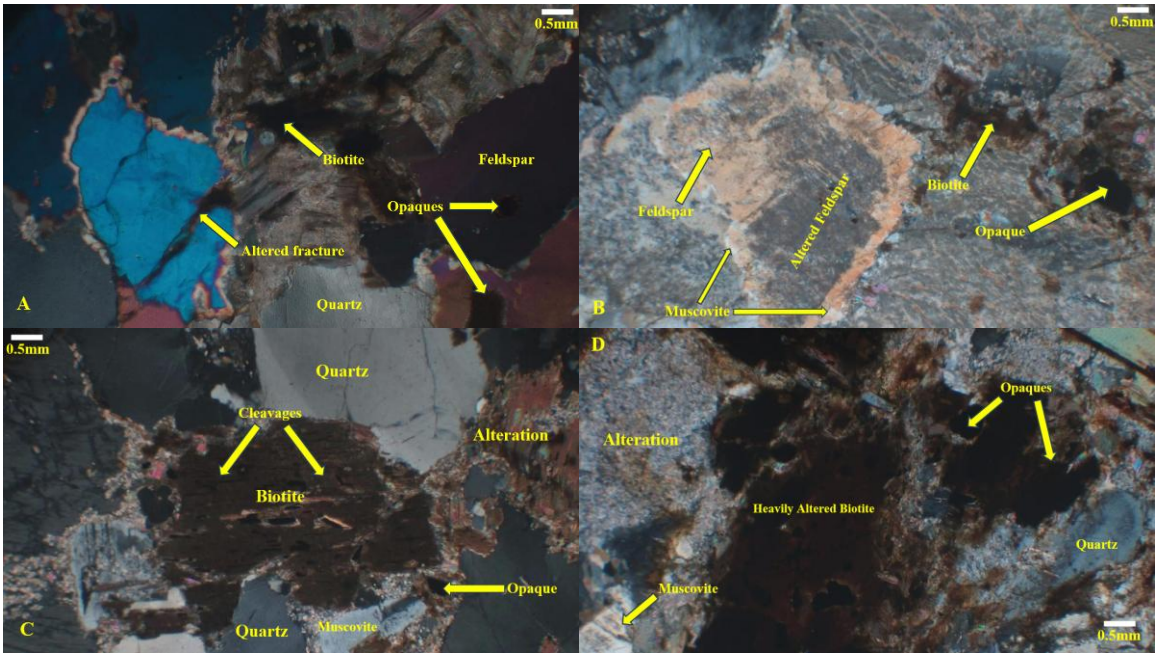


Figure 4.6 Representative photomicrographs of sample no. 6, (0.5mm), XPL, showing extensive biotite alteration and fractured quartz grains, thus having lower (MPa) values for UCS and SRH

CHAPTER 5

DISCUSSION

5.1 Discussion

The interpreted results of mechanical testing and petrography are discussed below in terms of correlations; they are as follows;

5.1.1 Correlation of mechanical tests with standards

The Schmidt Rebound Hammer (SRH) strength values and the directly measured Uniaxial Compressive Strength (UCS) values for all six Mansehra Granite specimens were assessed against three internationally recognized rock material strength classification schemes including; the Geological Society Engineering Group Working Party (1977), the International Association for Engineering Geology and the Environment (IAEG, 1977), and the International Society for Rock Mechanics (ISRM, 1981), to establish their classification positions under each standard and to evaluate the degree of agreement between the two testing methods.

When the SRH strength values, ranging from 52 MPa (S2) to 71 MPa (S1 and S5), are assessed against the Geological Society (1977) scheme, all six specimens fall uniformly within the Strong rock category (50–100 MPa). The IAEG (1977) classification produces an identical outcome, with all six MPa values falling within its Strong rock bracket (50–120 MPa). Under the ISRM (1981) scheme, however, the dataset divides across two categories: specimens S2 (52 MPa) and S3 (56 MPa) fall within the Moderate strength bracket (20–60 MPa), while S6, S4, S1, and S5, with strengths of 62, 66.8, 71, and 71 MPa respectively cross the 60 MPa threshold into the High strength bracket (60–200 MPa), making the ISRM (1981) the only scheme among the three to discriminate between specimens on the basis of the indirect test data.

When the directly measured UCS values, ranging from 124 MPa (S2) to 150 MPa (S1), are assessed against the same three schemes, a uniform one category upward shift is observed relative to the SRH based classifications. Under the Geological Society (1977) scheme, all six specimens move from strong into the Very Strong category (100–200 MPa), and under the IAEG (1977) scheme, all six similarly advance from strong into the Very Strong bracket (120–230 MPa). In correlation with ISRM (1981), all of the six specimens are categorized as high strength (60–200 MPa), bringing resolution the split produced by the indirect method and confirming that specimens S2 and S3, despite returning the lowest SRH values, are in fact high strength rocks when tested directly with uniaxial compressive strength test.

This discrepancy for S2 and S3 according to ISRM (1981), it is Moderate under indirect estimation (SRH) but High under direct measurement (UCS), and thus reflects the sensitivity of the Schmidt Rebound Hammer with regards to the surface conditions and local mineralogical variation at the point where the cylinder of hammer is applied, which can yield conservative strength estimates for granitic rocks being texturally heterogeneous (Aydin & Basu, 2005). Overall, the three classification schemes collectively confirm that the Mansehra Granite sampled in this study is a Strong to Very Strong, high integrity rock material under both indirect and direct testing methods, with

the direct UCS measurements consistently returning higher absolute values and higher classificatory positions across all three standards as shown in tables 5.1., 5.2., 5.3.

Direct correlation is also determined between UCS and Schmidt rebound values indicating that compressive strength is directly related to surface hardness as shown in table 5.4. and figure 5.1. The samples that have greater values of rebound tend to have greater values of UCS. This correlation proves that Schmidt hammer test can be utilized as a credible indirect technique of estimating rock strength, especially in initial studies.

Table 5.1 Standards of measurements for mechanical tests (Geological Society, 1977; IAEG, 1977; ISRM, 1981)

Geological Society	**UCS MPa**	**IAEG**	**UCS MPa**	**ISRM**	**UCS MPa**
Very weak	<1.25	Weak	<15	Very low	<6
Weak	1.25-5.00	Moderately weak	15-50	Low	6-10
Moderately weak	5.00-15.50	Strong	50-120	Moderate	20-60
Moderately strong	12.50-50	Very strong	120-130	High	60-200
Strong	50-100	Extremely Strong	Over 230	Very high	Over 200
Very strong	100-200	-	-	-	-
Extremely strong	Over 200	-	-	-	-

Table 5.2 UCS Test results of Mansehra Granite correlation with standard (Geological Society, 1977; IAEG, 1977; ISRM, 1981)

Sample No.	Peak Load (kN)	UCS (MPa)	Remarks
S1	356.37	150	Very Strong and High
S2	294.60	124	Very Strong and High
S3	301.70	127	Very Strong and High
S4	327.80	138	Very Strong and High
S5	344.50	145	Very Strong and High
S6	313.60	132	Very Strong and High

Table 5.3 SRH test results of Mansehra Granite correlated with standard (Geological Society, 1977; IAEG, 1977; ISRM, 1981)

Sample No.	Avg. Rebound Value	Strength (MPa)	Remarks
S1	53.0	71	Strong and High
S2	42.3	52	Strong and High
S3	44.2	56	Strong and High
S4	50.5	66.8	Strong and High

Sample No.	Avg. Rebound Value	Strength (MPa)	Remarks
S5	53.0	71	Strong and High
S6	46.6	62	Strong and High

Table 5.4 Correlation Between UCS and SRH of Mansehra Granite

Sample No.	UCS (MPa)	SRH Strength (MPa)
S1	150	71
S2	124	52
S3	127	56
S4	138	66.8
S5	145	71
S6	132	62

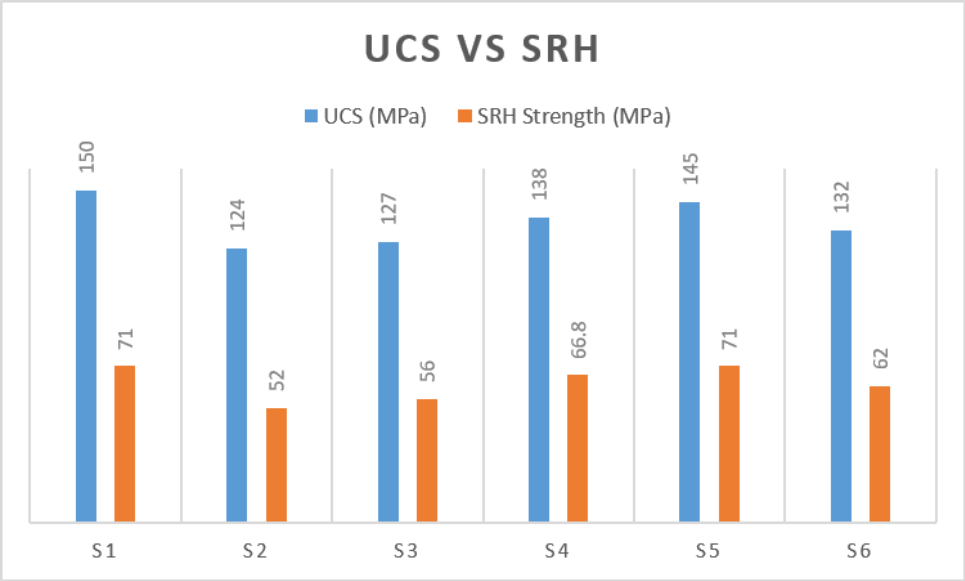


Figure 5.1 UCS (Mpa) vs SRH (Mpa) of Mansehra Granite

5.1.2 Correlation of mechanical tests with petrography

The petrographic analysis indicates that the Mansehra Granite is mainly composed of quartz, feldspar, and biotite. Quartz, which is a hard mineral, is also important in improving the overall strength of the rock. Feldspar is a constituent that contributes to the structural framework, and biotite is a constituent that occurs as a minor constituent and in some cases, may locally affect the mechanical behavior because of its cleavage and alteration tendencies.

The interlocking fabric is one of the major reasons why it has attained high mechanical strength and durability of the rock. The existence of minute micro fractures and localized change in the feldspar minerals explain slight variations of the mechanical properties of different samples.

The difference in engineering properties between samples is largely determined by the petrographic factors which include mineral composition, grain size, degree of alteration and presence of microfractures. The sample containing more quartz and well developed interlocking textures are higher in strength values, whereas minor changes and structural discontinuities can decrease the value of strength in small areas.

Table 5.5. has been utilized for plotting bar diagrams of UCS vs Petrography and SRH vs Petrography, as shown in figures 5.2., and 5.3. Direct relation has been observed between the Mpa values of UCS and SRH with petrography, wherein a higher value of UCS and SRH corresponds to a higher percentage of feldspar and quartz content in each of the samples.

Table 5.5 Modal mineralogy, UCS and SRH data of Mansehra Granite

Sample No.	UCS (MPa)	SRH (MPa)	Cumulative (%) Feldspars and Quartz
S1	150	71	88
S2	124	52	72
S3	127	56	77
S4	138	66.8	78
S5	145	71	81
S6	132	62	74

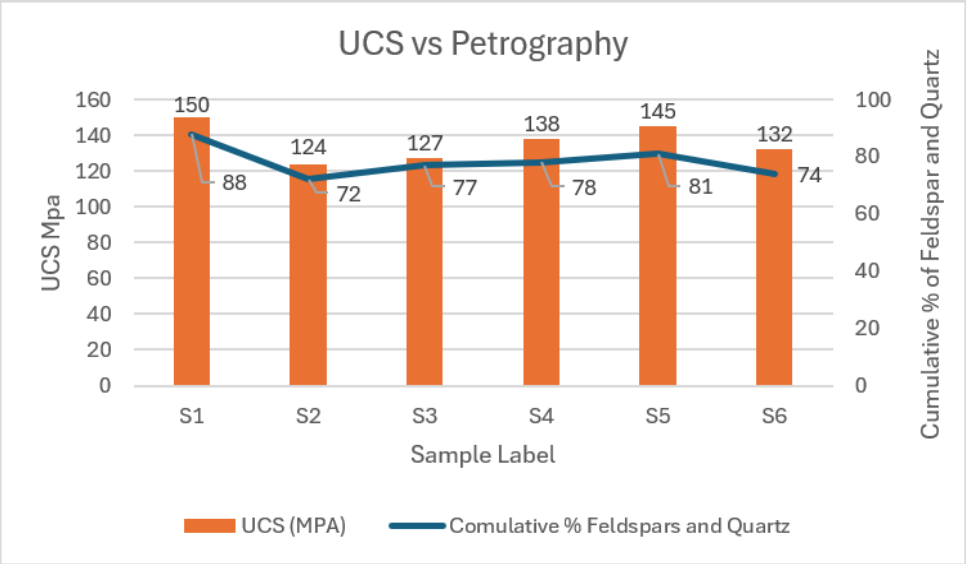


Figure 5.2 UCS (Mpa) vs Petrography (%) of Mansehra Granite

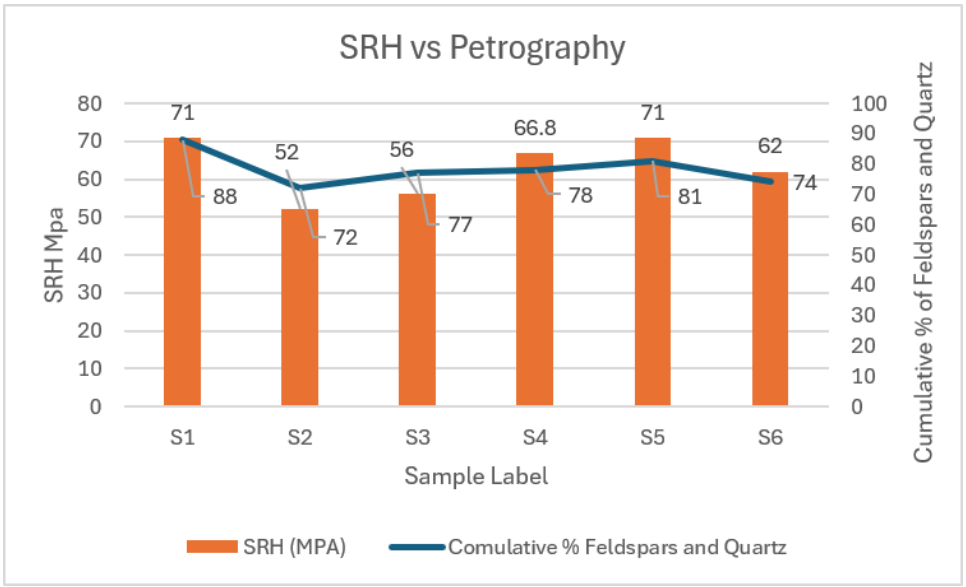


Figure 5.3 SRH (Mpa) vs Petrography (%) of Mansehra Granite

5.1.3 Influence of petrographic variability on geotechnical performance

Six specimens of the Mansehra Granite were characterized through integrated petrographic and geotechnical analysis, yielding UCS values of 124–150 MPa and SRH values of 52–71 MPa, classifying all specimens as Strong to Very Strong rock (Geological Society, 1977; IAEG, 1977), and High (ISRM, 1981). Regression analysis confirmed a strong SRH and UCS relationship ($R^2 = 0.9328$), a strong petrography and UCS dependence ($R^2 = 0.8276$), and a moderate petrography and SRH correlation ($R^2 = 0.6462$), establishing K feldspar abundance and low biotite content as the primary mineral scale controls on rock strength, with biotite alteration and Fe oxide precipitation as the principal factors governing inter sample variability.

5.1.4 Regression analysis

To quantify the relation between the measured geotechnical parameters and petrographic composition of Mansehra Granite, regression analysis was conducted on three pairs of variables: SRH versus UCS, UCS versus cumulative felsic index, and SRH versus cumulative felsic index. The strength and nature of the correlations between rock properties were statistically assessed using regression analysis, and the coefficient of determination (R^2) was adopted as the main goodness of fit measure.

Regression analysis conducted among the geotechnical and petrographic parameters of the Mansehra granite specimens revealed a strong and statistically significant relationship between Schmidt Rebound Hardness (SRH) and Uniaxial Compressive Strength (UCS) as shown in figure 5.4., yielding a coefficient of determination (R^2) of 0.9328. This near unity value confirms that SRH is a highly reliable nondestructive predictor of UCS for the Mansehra Granitic Complex and validates the

use of the Schmidt hammer as a field based strength estimation tool for this lithology. The regression of cumulative (quartz+feldspar %) against SRH (as shown in figure 5.5) gave a R^2 value of 0.6462, indicating a moderate correlation, suggesting that although petrographic composition is a factor influencing rebound values, surface irregularity, micro roughness and grain boundary conditions has an effect that cannot be fully explained by mineralogy alone when the cylinder reaches maximum. The regression of UCS against the petrographic cumulative index, however, yielded a much higher R^2 of 0.8276 as illustrated in figure 5.6. indicating that the bulk mineral composition has a much more significant control on UCS.

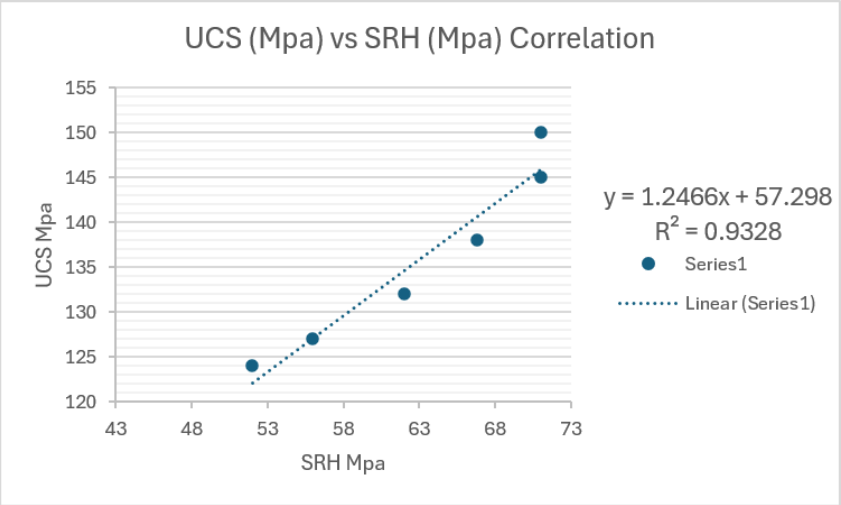


Figure 5.4 SRH (Mpa) vs UCS (Mpa) correlation of Mansehra Granite

R^2 value obtained from linear regression analysis of UCS (Mpa) and SRH (Mpa) is $R^2 = 0.9328$, which indicates a very strong correlation between them.

$$UCS = 1.2466(SRH) + 57.298$$

$$R^2 = 0.9328$$

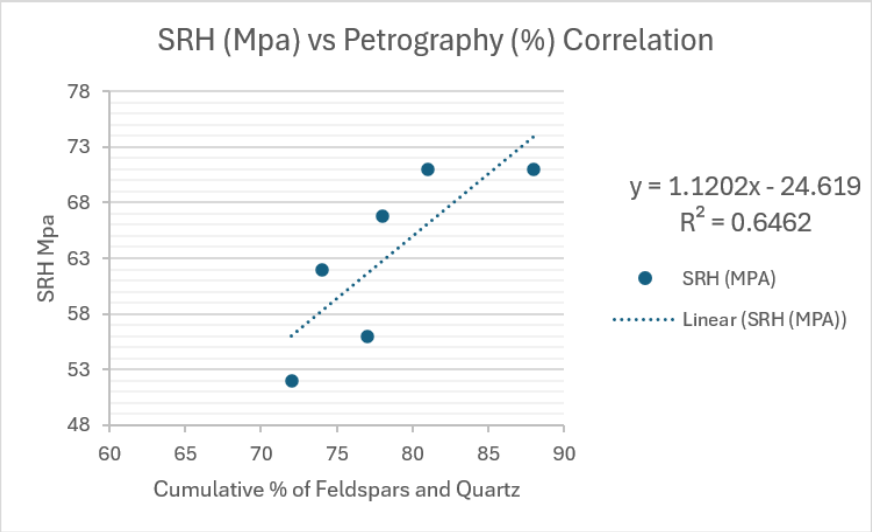


Figure 5.5 SRH (Mpa) vs Petrography (%) correlation of Mansehra Granite

R^2 value obtained from linear regression analysis of SRH (Mpa) and Petrography (%) is $R^2 = 0.6462$, which indicates a good correlation between them.

SRH = 1.1202(Petrography %) - 24.619

$R^2 = 0.6462$

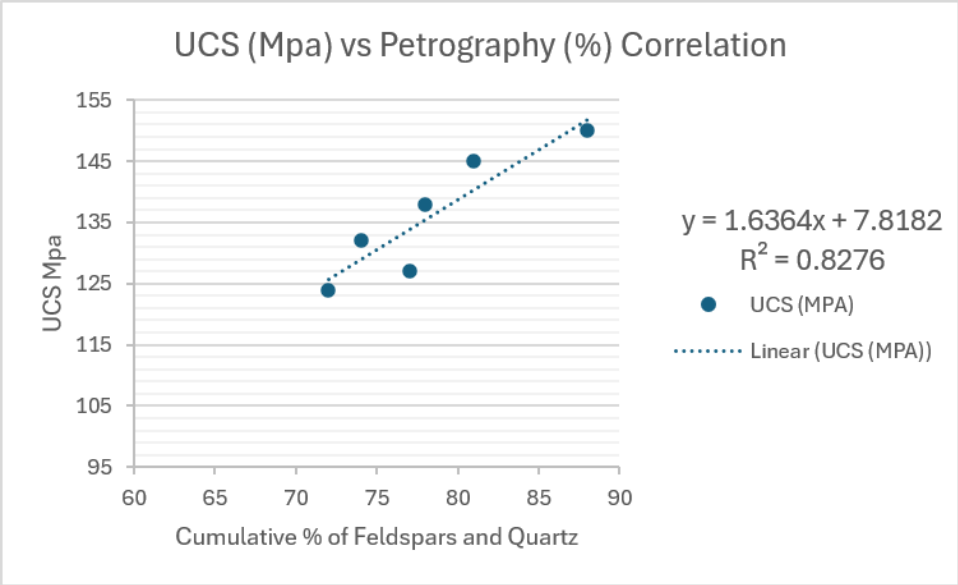


Figure 5.6 UCS (Mpa) vs Petrography (%) correlation of Mansehra Granite

R^2 value obtained from linear regression analysis of UCS (Mpa) and Petrography (%) is R^2 = 0.8276, which indicates a very good correlation between them.

UCS = 1.6364(Petrography %) + 7.8182

R^2 = 0.8276

The regression analysis and correlative analysis deemed Mansehra granite to be a very strong rock in general, but due to the small number of samples six (6), the data must be further validated by increasing the number of samples which will give a more accurate depiction of its strength, coupling this with the other parameters mentioned in the recommendations section will allow for a much better understanding of the degree of influence of petrography on strength of Mansehra granite.

CONCLUSIONS

This study demonstrates that the geotechnical behavior of the Mansehra Granitic Complex is fundamentally governed by mineralogy and deems it to be a very strong rock but the data must be further validated by increasing the number of samples. Sample S1, records the highest cumulative felsic proportion (88%), yielded the maximum UCS of 150 MPa and SRH of 71 MPa. Sample S5 closely followed with 81% cumulative felsic, producing UCS of 145 MPa and SRH of 71 MPa, confirming that an elevated quartz framework can compensate for low K-feldspar content. Sample S4 is distinguished by the highest plagioclase content (28%) among all specimens, achieved a UCS of 138 MPa and SRH of 66.8 MPa, indicating that plagioclase contributes meaningfully to compressive resistance when K feldspar is limited. Sample S6, with 74% cumulative felsic, yielded intermediate values of 132 MPa and 62 MPa, reflecting the competing effects of a moderate felsic framework against significant mafic alteration. Sample S3, despite carrying the highest individual quartz content (61%), recorded only 127 MPa and 56 MPa due to elevated biotite (14%) and advanced Fe oxide alteration reducing grain cohesion. Sample S2, with the lowest cumulative felsic proportion (72%) and joint highest biotite content (18%), produced the minimum UCS of 124 MPa and SRH of 52 MPa. Regression analysis confirmed a strong SRH vs UCS relationship ($R^2 = 0.9328$), a strong petrography to UCS dependence ($R^2 = 0.8276$), and a moderate petrography to SRH correlation ($R^2 = 0.6462$).

The correlations developed in the present study are directly applicable to the design and development of infrastructure in the entire Hazara Basin because the validated Schmidt Rebound Hardness as a field measurement of UCS will minimize the need for extensive laboratory testing during preliminary site investigations in the remote

Himalayan terrain. The petrographic and UCS regression further validates the use of modal mineralogy from thin section analysis as a predictive tool for compressive strength, offering a practical way for engineers to characterize the Mansehra Granite at unexplored localities. The baseline dataset developed during this study will provide a critical baseline for material suitability evaluations and foundation design in the region, where construction materials are increasingly needed and where infrastructure development is underway in the form of road networks, hydropower projects, and slope stabilization works. The methodology used here, in turn, offers a replicable approach to geotechnical characterization of other data-poor granitic areas in northern Pakistan.

RECOMMENDATIONS

Future research should focus on increasing the sample population beyond the six bulk specimens analyzed in this study to incorporate samples from various weathering grades, lithological variants and structural zones throughout the Hazara Basin to encompass the full geomechanical range of the Mansehra Granitic Complex. This work was done through visual estimations for modal mineralogy thus point counting should be performed for future work using quantitative image analysis software instead of manual techniques to avoid observer bias and to enhance the reproducibility of the results. The future investigation should also incorporate a wider range of geomechanical parameters such as tensile strength from the Brazilian disc test, point load index, ultrasonic pulse velocity, specific gravity, water absorption and porosity measurements, and provide a comprehensive multi-parameter geomechanical model that can support rock mass classification in the RMR and Q-systems.

Lastly, petrographic mapping of the zones throughout the complex, combined with field based Schmidt hammer surveys, would allow for spatial prediction of rock quality to aid in engineering site selection, material sourcing, and geohazard assessment across the Hazara Basin.

REFERENCES

Anees, M., Wajid, A. A., Qureshi, A. A., Jadoon, I. A. K., Manzoor, S., Atique, A., & Masood, A. (2016). Study of textural and petrographic features in Mansehra Granite, Pakistan: Implications on gamma radioactivity and dose rates. The Nucleus, 53(1), 38–48.

Arif, M., Mulk, A., Mehmood, M. T., & Shah, S. M. H. (1999). Petrography and mechanical properties of the Mansehra Granite, Hazara, Pakistan. Geological Bulletin, University of Peshawar, 32, 41–49.

ASTM International. (1995). Standard test method for unconfined compressive strength of intact rock core specimens (ASTM D 2938-95). ASTM International.

ASTM International. (2000). Standard test method for determination of rock hardness by rebound hammer (ASTM D 5873-00). ASTM International.

ASTM International. (2014). Standard practice for rock core drilling and sampling of rock for site exploration (ASTM D 2113-14). ASTM International.

ASTM International. (2019). ASTM C295/C295M-19: Standard guide for petrographic examination of aggregates for concrete. ASTM International.

ASTM International. (2019). Standard practices for preparing rock core as cylindrical test specimens and verifying conformance to dimensional and shape tolerances (ASTM D 4543-19). ASTM International.

ASTM International. (2019). Standard practices for preserving and transporting rock core samples (ASTM D 5079-19). ASTM International.

Awan, R. S., Khan, A., Liu, C., Yang, S., Zang, Q., Wu, Y., Li, G., Iltaf, K. H., Tahir, M. and Ali, S. (2021). Subsurface geological model of sedimentary and metasedimentary wedge from Mansehra to Battal based on gravity data, Hazara area, Pakistan. Energy Geoscience, 2(4), 229-237.

Aydin, A., & Basu, A. (2005). The Schmidt hammer in rock material characterization. Engineering Geology, 81(1), 1–14.

Barton, N., Lien, R., & Lunde, J. (1974). Engineering classification of rock masses for the design of tunnel support. Rock Mechanics, 6(4), 189–236.

Bell, F. G. (2007). Engineering geology (2nd ed.). Butterworth-Heinemann.

Bieniawski, Z. T. (1989). Engineering rock mass classifications: A complete manual for engineers and geologists in mining, civil, and petroleum engineering. John Wiley & Sons.

Bossart, P., Dietrich, D., Greco, A., Ottiger, R., & Ramsay, J. G. (1988). The tectonic structure of the Hazara–Kashmir Syntaxis, southern Himalayas, Pakistan. Tectonics, 7(2), 273–297.

Broch, E., & Franklin, J. A. (1972). The point-load strength test. International Journal of Rock Mechanics and Mining Sciences & Geomechanics Abstracts, 9(6), 669–676.

Brown, E. T. (Ed.). (1981). Rock characterization, testing and monitoring: ISRM suggested methods. Pergamon Press.

Bureau of Indian Standards. (1992). Method of non-destructive testing of concrete: Part 2 rebound hammer (IS 13311, Part 2). Bureau of Indian Standards.

Colback, P. S. B., & Wiid, B. L. (1965). The influence of moisture content on the compressive strength of rocks. In Proceedings of the 3rd Canadian Rock Mechanics Symposium (pp. 65–83). University of Toronto.

DiPietro, J. A., & Pogue, K. R. (2004). Tectonostratigraphic subdivisions of the Himalaya: A view from the west. Tectonics, 23(5), TC5001.

DiPietro, J. A., Ahmad, I., & Hussain, A. (2021). Geologic history and thermal evolution in the hinterland region, western Himalaya, Pakistan. Earth-Science Reviews, 220, 103742.

Engineering and General Geology Singh, P. (2005). Engineering and General Geology. S.K. Kataria & Sons, New Delhi.

Engineering Properties of Rocks Goodman, R. E. (1989). Introduction to Rock Mechanics (2nd ed.). Wiley.

Engineering Rock Mechanics Hudson, J. A., & Harrison, J. P. (1997). Engineering Rock Mechanics: An Introduction to the Principles. Elsevier Science Ltd.

Geological Society Engineering Group Working Party. (1977). The description of rock masses for engineering purposes. Quarterly Journal of Engineering Geology, 10(4), 355–388.

Hawkins, A. B. (1998). Aspects of rock strength. Bulletin of Engineering Geology and the Environment, 57(1), 17–30.

Hoek, E., & Bray, J. D. (1981). *Rock slope engineering*. CRC press.

Hoek, E., & Brown, E. T. (1980). Underground excavations in rock. Institution of Mining and Metallurgy.

Hoek, E., Carranza-Torres, C., & Corkum, B. (2002). Hoek–Brown failure criterion—2002 edition. In Proceedings of the 5th North American Rock Mechanics Symposium (Vol. 1, pp. 267–273). University of Toronto Press.

Hudson, J. A., & Harrison, J. P. (1997). Engineering rock mechanics: An introduction to the principles. Pergamon Press.

International Association for Engineering Geology and the Environment. (1977). Recommended rock and soil description. Bulletin of the International Association of Engineering Geology, 16, 151–156.

International Society for Rock Mechanics (1981). Rock Characterization, Testing and Monitoring – ISRM Suggested Methods. Pergamon Press, Oxford.

International Society for Rock Mechanics. (1978). Suggested methods for the quantitative description of discontinuities in rock masses. International Journal of Rock Mechanics and Mining Sciences & Geomechanics Abstracts, 15(6), 319–368.

Iqbal, A., Ali Khan, M., Kontakiotis, G., Aamir, H. M., Ahmed, I., Besiou, E. and Antonarakou, A. (2026). Sedimentology and Geochemistry of the Early Cambrian Hazira Formation in the Haripur Region, Lesser Himalayas, Pakistan. Russian Geology and Geophysics.

Jaeger, C. (1972). Rock mechanics and engineering. Cambridge University Press.

Jan, M. Q., Kempe, D. R. C., & Tahirkheli, R. A. K. (1981). The geology and petrography of the Tarbela "alkaline" complex. Geological Bulletin, University of Peshawar, 14, 1–28.

Khan, H., & Sajid, M. (2023). Investigating the textural and physico-mechanical response of granites to heat treatment. International Journal of Rock Mechanics and Mining Sciences, 161, 105281.

Le Fort, P., Debon, F., & Sonet, J. (1980). The "Lesser Himalayan" cordierite granite belt: Typology and age of the pluton of Mansehra (Pakistan). Geological Bulletin, University of Peshawar, 13(Special Issue), 51–62.

Le Fort, P., Debon, F., & Sonet, J. (1983). The Lower Paleozoic "Lesser Himalayan" granitic belt: Emphasis on the Simchar Pluton of Central Nepal. In F. A. Shams (Ed.), Granites of Himalaya, Karakoram and Hindukush (pp. 235–255). Institute of Geology, Punjab University.

Le Fort, P., Debon, F., Pêcher, A., Sonet, J., & Vidal, P. (1986). The 500 Ma magmatic event in Alpine southern Asia: A thermal episode at Gondwana scale. Sciences de la Terre, Mémoires, 47, 191–209.

Marinos, P., & Hoek, E. (2000). GSI: A geologically friendly tool for rock mass strength estimation. In Proceedings of the GeoEng2000 Conference (pp. 1422–1442). Technomic Publishing.

Naeem, M., Burg, J.-P., Ahmad, N., Chaudhry, M. N., & Khalid, P. (2016). U-Pb zircon systematics of the Mansehra Granitic Complex: Implications on the early Paleozoic orogenesis in NW Himalaya of Pakistan. Geosciences Journal, 20(4), 427–447.

Naeem, M., Burg, J.-P., Ahmad, N., Chaudhry, M. N., & Khalid, P. (2021). Mineralogy and geochemistry of calc-alkaline magmatic rocks from the Mansehra Granitic Complex, NW Himalaya, Pakistan: Insights into petrogenesis and tectonic setting. Arabian Journal of Geosciences, 14(14), 1383.

Naeem, M., Khalid, P., & Anwar, A. W. (2015). Construction material prospects of granitic and associated rocks of Mansehra area, NW Himalaya, Pakistan. Acta Geodaetica et Geophysica, 50(3), 307–319.

Ogasawara, M., Naeem, M., & Yamamoto, T. (2019). Origin of the Ordovician Mansehra granite in the NW Himalaya, Pakistan: Constraints from Sr–Nd isotopic data, zircon U–Pb age and Hf isotopes. In R. Sharma & I. M. Villa (Eds.), Crustal architecture and evolution of the Himalaya–Karakoram–Tibet Orogen (pp. 97–120). Geological Society, London, Special Publications, 481.

Pogue, K. R., Wardlaw, B. R., Harris, A. G., & Hussain, A. (1999). Paleozoic and Mesozoic stratigraphy of the Peshawar Basin, Pakistan: Correlations and implications. Geological Society of America Bulletin, 111(5), 699–718.

Qasim, M., Ahmad, J., Ding, L., & Khan, M. A. (2023). Sedimentological and petrographical characterization of the Cambrian Abbottabad Formation in Kamsar section, Muzaffarabad area: Implications for Proto-Tethys Ocean evolution. Journal of Marine Science and Engineering, 11(3), 526.

Qasim, M., Khan, M. A., & Haneef, M. (2014). Stratigraphic characterization of the Early Cambrian Abbottabad Formation in the Sherwan area, Hazara region, N. Pakistan:

Implications for Early Paleozoic stratigraphic correlation in NW Himalayas, Pakistan. Journal of Himalayan Earth Sciences, 47(1), 25–40.

Qasim, M., Khan, M. A., & Haneef, M. (2015). Stratigraphic characterization and structural analysis of the northwestern Hazara Ranges across Panjal Thrust, northern Pakistan. Arabian Journal of Geosciences, 8(9), 7011–7030.

Sajid, M., & Arif, M. (2015). Reliance of physico-mechanical properties on petrographic characteristics: Consequences from the study of Utla Granites, north-west Pakistan. Bulletin of Engineering Geology and the Environment, 74(4), 1321–1330.

Sajid, M., Andersen, J., Rocholl, A., & Wiedenbeck, M. (2018). U-Pb geochronology and petrogenesis of peraluminous granitoids from northern Indian plate in NW Pakistan: Andean-type orogenic signatures from the early Paleozoic along the northern Gondwana. Lithos, 318, 340–356.

Sajid, M., Coggan, J., Arif, M., Andersen, J., & Rollinson, G. (2016). Petrographic features as an effective indicator for the variation in strength of granites. Engineering Geology, 202, 44–54.

Streckeisen, A. (1976). To each plutonic rock its proper name. Earth-Science Reviews, 12(1), 1–33.

Terzaghi, K. (1943). Theoretical soil mechanics. John Wiley & Sons.

Tugrul, A., & Zarif, I. H. (1999). Correlation of mineralogical and textural characteristics with engineering properties of selected granitic rocks from Turkey. Engineering Geology, 51(4), 303–317.

Umar, M., Sabir, M. A., Farooq, M., Khan, M. M. S. S., Faridullah, F., Jadoon, U. K., & Khan, A. S. (2015). Stratigraphic and sedimentological attributes in Hazara Basin Lesser Himalaya, North Pakistan: their role in deciphering minerals potential. Arabian Journal of Geosciences, 8(3), 1653-1667.

Zafar, T., Mahar, M. A., Rehman, H. U., Riaz, M., Latif, K., Oyebamiji, A., & Naeem, M. (2019). Geochemical and petrological characteristics of xenoliths in Mansehra Granite, NW Himalaya, Pakistan: Implications for petrogenesis and tectonic settings. Episodes, 42(4), 263–285.

Suleman Gul Khan MS Thesis Geology

ORIGINALITY REPORT

15%	8%	14%	4%
SIMILARITY INDEX	INTERNET SOURCES	PUBLICATIONS	STUDENT PAPERS

PRIMARY SOURCES

1	Rizwan Sarwar Awan, Ashar Khan, Chenglin Liu, Shangfeng Yang et al. "Subsurface geological model of sedimentary and metasedimentary wedge from Mansehra to Battal based on gravity data, Hazara area, Pakistan", Energy Geoscience, 2021 Publication	2%
2	www.researchgate.net Internet Source	2%
3	Submitted to Higher Education Commission Pakistan Student Paper	1%
4	Mustansar Naeem, Jean-Pierre Burg, Nasir Ahmad, Muhammed Nawaz Chaudhry, Perveiz Khalid. "U-Pb zircon systematics of the Mansehra Granitic Complex: implications on the early Paleozoic orogenesis in NW Himalaya of Pakistan", Geosciences Journal, 2016 Publication	1%
5	www.irsm.cas.cz Internet Source	1%
6	Jaak J.K. Daemen, Richard A. Schultz. "Rock Mechanics Proceedings of the 35th U.S. Symposium", CRC Press, 2026 Publication	<1%
7	Khan, Assad. "Petrogenetic and Geochemical Characterization of the Spinghar Crystalline Complex in North-Western Pakistan", University of South Wales (United Kingdom), 2024 Publication	<1%
8	discovery.researcher.life Internet Source	<1%
9	Nick Barton, Ove Stephansson. "Rock Joints - Proceedings of the International Symposium on Rock Joints Loen / Norway / 4-6 June 1990", CRC Press, 2026 Publication	<1%
10	www.mdpi.com Internet Source	<1%
11	Muhammad Qasim, Muhammad Asif Khan, Muhammad Haneef. "Stratigraphic characterization and structural analysis of the northwestern Hazara Ranges across Panjal Thrust, northern Pakistan", Arabian Journal of Geosciences, 2015	<1%

	Publication	
12	M Arif, M Ashraf, MS Baig, GH McNally, FL Roberts, FA Shams. "Construction material prospects of granitic and associated rocks of Mansehra area, NW Himalaya, Pakistan", 'Springer Science and Business Media LLC' Internet Source	<1 %
13	Malik Muhammad Saud Sajid Khan, Muhammad Umar, Bing Pan, Xiaojuan Sun et al. "A newly discovered Neoproterozoic diamictite-cap carbonate couplet from the Western Himalaya: The expansion of the Marinoan snowball Earth glaciation to the northwestern margin of the Indian Plate in North Pakistan", Precambrian Research, 2022 Publication	<1 %
14	Yadav, Binod Kumar. "Interval Finite Element Approach for Stability Analysis of Concrete Gravity Dams Under Uncertainties.", Georgia Institute of Technology Publication	<1 %
15	www.ijraset.com Internet Source	<1 %
16	ntnuopen.ntnu.no Internet Source	<1 %
17	Submitted to A'Sharqiyah University, Oman Student Paper	<1 %
18	K.P. Arandara, G.N. Paranavithana, S.T. Priyadarshana, H.M.T.G.A. Pitawala, R. Dissanayake. "Evaluation of coconut shell biochar on recycled aggregate concrete through petrographic studies", Construction and Building Materials, 2024 Publication	<1 %
19	journalijsra.com Internet Source	<1 %
20	Qin, . "Experiments", Mechanics of Cellular Bone Remodeling Coupled Thermal Electrical and Mechanical Field Effects, 2013. Publication	<1 %
21	Tariq Mahmood, Naveed Ahsan, Muhammad Armaghan Faisal Miraj. "Depositional cyclicity of lower Cambrian strata in the NW Himalayas: Regional sequence stratigraphy of the Indian passive margin", Marine and Petroleum Geology, 2024 Publication	<1 %
22	fdocuments.net Internet Source	<1 %
23	D.G. Price. "Proceedings Sixth International Congress International Association of Engineering Geology - 6-10 August 1990 / Amsterdam / Netherlands", CRC Press,	<1 %

	2026 Publication	
24	Shihong Tian, Zengqian Hou, Xinyang Chen, Hengci Tian, Yingli Gong, Zhusen Yang, Tianyi Huang, Xianfang Li, Xuanxue Mo. "Magnesium isotopic behaviors between metamorphic rocks and their associated leucogranites, and implications for Himalayan orogenesis", Gondwana Research, 2020 Publication	<1 %
25	www.wrc.org.za Internet Source	<1 %
26	Kallu, Raj, and Pedram Roghanchi. "Correlations between direct and indirect strength test methods", International Journal of Mining Science and Technology, 2015. Publication	<1 %
27	Phillipson, S.E.. "Texture, mineralogy, and rock strength in horizontal stress-related coal mine roof falls", International Journal of Coal Geology, 20080805 Publication	<1 %
28	Submitted to University of South Africa Student Paper	<1 %
29	infostore.saiglobal.com Internet Source	<1 %
30	"Soft Rock Mechanics and Engineering", Springer Science and Business Media LLC, 2020 Publication	<1 %
31	d-nb.info Internet Source	<1 %
32	server1.madcad.com Internet Source	<1 %
33	worldwidescience.org Internet Source	<1 %
34	Farquharson, Robin Bruce. "Whole-Rock Isotopic Studies in the Region of Mount Isa, Queensland", The Australian National University (Australia), 2021 Publication	<1 %
35	Shuja Ullah, Nazir Ur Rehman, Abdul Rahim Asif, Rizwan Ullah, Liaqat Ali, Muhammad Rizwan, Faheem Ahmed, Tanzeel Ur Rehman. "Engineering properties assessment and aggregate suitability of the jurassic and eocene limestone: a case study from the Upper Indus Basin, Pakistan", Carbonates and Evaporites, 2024 Publication	<1 %

36	Submitted to University of Sheffield Student Paper	<1%
37	A. Wolter, V. Gischig, D. Stead, J. J. Clague. "Investigation of Geomorphic and Seismic Effects on the 1959 Madison Canyon, Montana, Landslide Using an Integrated Field, Engineering Geomorphology Mapping, and Numerical Modelling Approach", Rock Mechanics and Rock Engineering, 2015 Publication	<1%
38	John F. Cassidy. "Chapter 102 Earthquake Magnitude", Springer Science and Business Media LLC, 2018 Publication	<1%
39	Joseph A. DiPietro. "Geologic map of the Indus syntaxis and surrounding area, northwest Himalaya, Pakistan", Special Paper 328 Himalaya and Tibet Mountain Roots to Mountain Tops, 1999 Publication	<1%
40	Muhammad Qasim, Lin Ding, Muhammad Asif Khan, Ishtiaq A. K. Jadoon et al. "Tectonic Implications of Detrital Zircon Ages From Lesser Himalayan Mesozoic-Cenozoic Strata, Pakistan", Geochemistry, Geophysics, Geosystems, 2018 Publication	<1%
41	ebin.pub Internet Source	<1%
42	econ-environ-geol.org Internet Source	<1%
43	"Cenozoic kinematic history of the Kohistan fault in the Pakistan Himalaya", Geological Society of America Bulletin, 2008 Publication	<1%
44	F.G. Bell. "ENGINEERING GEOLOGY | Rock Properties and Their Assessment", Elsevier BV, 2005 Publication	<1%
45	Joseph A. DiPietro, Alex Pullen, Michael A. Krol. "Geologic history and thermal evolution in the Hinterland Region, Western Himalaya, Pakistan", Earth-Science Reviews, 2021 Publication	<1%
46	Muhammad Umar, Muhammad Amjad Sabir, Muhammad Farooq, Malik Muhammad Saud Sajid Khan et al. "Stratigraphic and sedimentological attributes in Hazara Basin Lesser Himalaya, North Pakistan: their role in deciphering minerals potential", Arabian Journal of Geosciences, 2014 Publication	<1%

47	Musa Khan, Rehan Khan, Shams Ul Islam, Asad Khan, Yanmei Zhong, Fuad A. Awwad, Emad A.A. Ismail. "Provenance, diagenesis, and depositional environment of Miocene Kamlial Formation, Azad Jammu and Kashmir, Sub Himalayas, Pakistan: Evidences from field observations and petrography", Heliyon, 2024 Publication	<1 %
48	W. Joel Schiffer, Delores M. Robinson, Shah Faisal, Harold H. Stowell. "Exploring the tectonostratigraphy of the Pakistan Himalaya with new detrital zircon geochronology and neodymium isotope data from the Kaghan Valley", Geoscience Frontiers, 2023 Publication	<1 %
49	etheses.dur.ac.uk Internet Source	<1 %
50	inonreivoi.web.app Internet Source	<1 %
51	unsworks.unsw.edu.au Internet Source	<1 %
52	xfer.services.ncdot.gov Internet Source	<1 %
53	docslib.org Internet Source	<1 %
54	en.earth-science.net Internet Source	<1 %
55	pure.royalholloway.ac.uk Internet Source	<1 %
56	sutir.sut.ac.th:8080 Internet Source	<1 %
57	Abdelkarim Ait Baha, Isma Amri, Muhammad Ouabid, Khalil El Kadiri et al. "Petrographic, physical–mechanical and fracture modeling of granites: an integrated approach to evaluating the stone reserves and mineral deposits of Ment Granite (western Meseta, Central Massif of Morocco)", Bulletin of Engineering Geology and the Environment, 2025 Publication	<1 %
58	B.K. Chakrabarti. "Pakistan Himalaya", Elsevier BV, 2026 Publication	<1 %
59	Hi-Keun Lee, Hyung-Sik Yang, So-Keul Chung. "Environmental and Safety Concerns in Underground Construction", CRC Press, 2026 Publication	<1 %

60	Mamdouh E. Osman, Ashraf M. Osman, Nabil M. Nagy, Ismail M. Kamal. "Comparative application of different rock mass classification systems for determining rock mass properties and support design for a tunnel in weak rock: a case study", Innovative Infrastructure Solutions, 2026 Publication	<1 %
61	R. J. Watters, D. R. Zimbelman, S. D. Bowman. "Rock Mass Strength Assessment and Significance to Edifice Stability, Mount Rainier and Mount Hood, Cascade Range Volcanoes", Pure and Applied Geophysics, 2000 Publication	<1 %
62	Youngquist, Leah. "Microstructural Controls on Macroscopic Processes from the Perspective of Deformation in Convergent Margins.", The Pennsylvania State University Publication	<1 %
63	link.springer.com Internet Source	<1 %
64	www.iaeg.info Internet Source	<1 %
65	J. S. Moore. "FIELD PROCEDURES FOR THE HEADCUT ERODIBILITY INDEX", Transactions of the ASAE, 1997 Publication	<1 %
66	Michael A. Murphy. "Transtensional deformation in the central Himalaya and its role in accommodating growth of the Himalayan orogen", Tectonics, 2005 Publication	<1 %
67	Muhammad Qasim, Lin Ding, Muhammad Asif Khan, Muhammad Umar et al. "Late Neoproterozoic-Early Palaeozoic stratigraphic succession, Western Himalaya, North Pakistan: Detrital zircon provenance and tectonic implications", Geological Journal, 2017 Publication	<1 %
68	Yang, J.H.. "Petrogenesis of Early Cretaceous intrusions in the Sulu ultrahigh-pressure orogenic belt, east China and their relationship to lithospheric thinning", Chemical Geology, 20051105 Publication	<1 %

Exclude quotes	Off	Exclude matches	Off
Exclude bibliography	Off		